This project is funded by the Horizon 2020 Framework Program of the European Union

Built2Spec

Built to Specifications – Tools for the 21st Century Construction Site

H2020Grant Agreement – 637221

D3.11 Parametric loudspeaker lab-test results

Primary Author: La Salle, Universitat Ramon Llull

Marc Arnela, Oriol Guasch, Patricia Sánchez-Martín, Carme Martínez and Umut Sayin

1st Quality reviewer: Marc Arnela

2nd Quality reviewer: Aurélien Henon

Deliverable nature:	Report (R)
Dissemination level: (Confidentiality)	Public (PU)
Contractual delivery date:	**M27** –March 31th, 2017
Actual delivery date:	
Version:	1.1
Total number of pages:	46
Keywords:	Acoustics, Omnidirectional Parametric Loudspeaker

DISCLAIMER

ACKNOWLEDGEMENT

This document is a deliverable of the BUILT2SPEC project which has received funding from theEuropean Union's Horizon 2020 Research and Innovation Program under Grant Agreement no. 637221.

Executive summary

The **Deliverable D3.11** entitled "Parametric loudspeaker lab-test results" is a public document delivered in the context of WP3, Task 3.3: Acoustics. The deliverable is authored by the following researchers: Marc Arnela, Oriol Guasch, Patricia Sánchez-Martín, Carme Martínez and Umut Sayin.

This work is part of the project on Tools for the 21st Century Construction Worksite (BUILT2SPEC) and is financed by the European Union under the Horizon 2020 Program.

This deliverable D3.11 presents in detail the experimental measurements performed for the design and testing of an omnidirectional parametric loudspeaker (OPL) prototype that generates audible sound through hundreds of ultrasound transducers set on a sphere. Several commercial ultrasound transducers could be used for this purpose, but not all of them may fit the design requirements. An extensive campaign of measurements was first performed to select a set of possible candidates. Based on the obtained results, a first OPL prototype was designed and built. The design and construction details are described in the companion deliverable D3.10 "Parametric loudspeaker prototypes" as well as the criterion used to select the ultrasound transducer. Different measurements were then performed to test this first OPL prototype, which include the frequency response, directivity, and sound pressure levels, among others. However, the obtained results were not as expected. Although a flat frequency response was obtained, the sound pressure levels were not loud enough. Moreover, this first OPL prototype was not as omnidirectional as one would desire. A second OPL prototype was then designed using an improved theoretical model (described in the deliverable D3.10), which required collecting new experimental data for three different ultrasound transducers. The second OPL prototype is currently under construction, but similar tests than those performed for the first OPL prototype will be performed to characterize it, as well as to compare it with the prediction theoretical model.

This document is structured as follows:

- First, the results obtained for the first measurement campaign of ultrasound transducers are presented. These results are used to select the best transducer for building the first OPL prototype, the OPL#1.
- The OPL#1 is then characterized to obtain the frequency response, the directivity, and the sound pressure levels in free-field and diffuse field conditions.
- Given that the acoustic response of the OPL#1 was not as good as expected, a second prototype, the OPL#2, was designed with an improved theoretical model. To do so, a new campaign of measurements was carried out, which is herein described. Moreover, comparisons between theoretical results and experiments are also provided.

1 TABLE OF CONTENT

Abbreviations

B2S = Built to Specifications

WP = Work Package;

OPL = Omnidirectional Parametric Loudspeaker;

SPL = Sound Pressure Level;

PAA = parametric acoustic array;

USBAM = Upper Side Band Amplitude Modulation.

2 Introduction

Omnidirectional sound sources are acoustic devices that radiate sound waves in all directions. They are needed to evaluate the acoustic performance of buildings. Some examples are the measurement of airborne sound insulation, reverberation time, and speech intelligibility. They have typically been constructed by setting 12 regular loudspeakers in a dodecahedral configuration (see Figure 2.1), although any other polyhedron could also be used. Each loudspeaker radiates sound waves resulting in a spherical pattern. However, the higher the frequency, the more directive a regular loudspeaker is, losing this omnidirectional behaviour, especially at the edges between neighbouring loudspeaker. Moreover, dodecahedral sources are quite big and heavy (about 8 kg), which makes difficult to carry them.

In the frame of B2S we aim at building a light omnidirectional sound source that could circumvent the directivity problems of the standard sources. The idea is to replace the standard loudspeakers by hundreds of ultrasound transducers (see Figure 2.1). These transducers emit a very directive ultrasonic beam containing the audible signal modulated with a carrier. Thanks to the non-linear propagation of sound in air, the air itself demodulates the signal, bringing it back to the audible range. Ideally, with a high enough density of transducers a very omnidirectional behaviour should be achieved. Moreover, these transducers are very light compared to regular loudspeakers, which should largely reduce the total weight. This source of sound based on ultrasound transducers will be hereafter referred as the omnidirectional parametric loudspeaker (OPL), since the technology behind it is that of parametric acoustic arrays (PAA).

Several ultrasound transducers are available in the market, and not all of them may fit the requirements of an OPL. First, in Section 3 the behaviour of different transducers is measured in lab conditions, from which one transducer is selected to build the first OPL prototype, the OPL#1. In the following Section 4 the OPL#1 is tested to evaluate the generated Sound Pressure Levels (SPL) and the directivity pattern, among other proprieties. Unfortunately, the results for the OPL #1 were not as good as expected, so it was decided to build a second OPL prototype, the OPL#2. Section 5 shows the results of a new measurement campaign of ultrasound transducers needed for the design of the OPL#2, and also presents some comparisons with an improved theoretical model.

Figure 2.1. (Right) Standard omnidirectional sound source and (left) proposed omnidirectional parametric loudspeaker (OPL).

3 Characterization of ultrasound transducers for the OPL#1

3.1 Introduction

Different commercial ultrasound transducers in the market were selected as candidates for the first OPL prototype (OPL#1). Several measurements were performed to obtain the frequency response, the directivity, and maximum audible level produced at different angles.

The following ultrasound transducers were tested:

- **Murata 10mm (MA40S4S):** transmitter with a 10mm diaphragm. Plastic cover.
- **Multicomp 10mm (ST100):** transmitter with a 10mm diaphragm. Plastic cover.
- **Prowave 10mm (400ST100):** transmitter with a 10mm diaphragm. Aluminium cover.
- **Prowave 12mm (400ST120):** transmitter with a 12mm diaphragm. Aluminium cover.
- **Multicomp 16mm Transciever (PT160):** transceiver with a 16mm diaphragm. Plastic cover.
- **Multicomp 16mm Transmitter (ST160):** transmitter with a 16mm diaphragm. Plastic cover.
- **Prowave 16mm (400ST160):** transmitter with a 16mm diaphragm. Aluminium cover.

3.2 Experimental setup

The transducers were tested in the anechoic room of La Salle, Universitat Ramon Llull (see Figure 3.1). Sinusoidal signals with third octave central frequencies from 20 Hz to 20 kHz were modulated with Upper Side Band Amplitude Modulation (USBAM) and emitted as test signals trough a Data Translation 9832 card. These signals were next amplified with an Ecler XPA3000, adjusting the output level to have a voltage of 19.75V_{rms}. This value was selected not to overcome the maximum voltage of 20 V_{rms} than an ultrasound transducer admits.

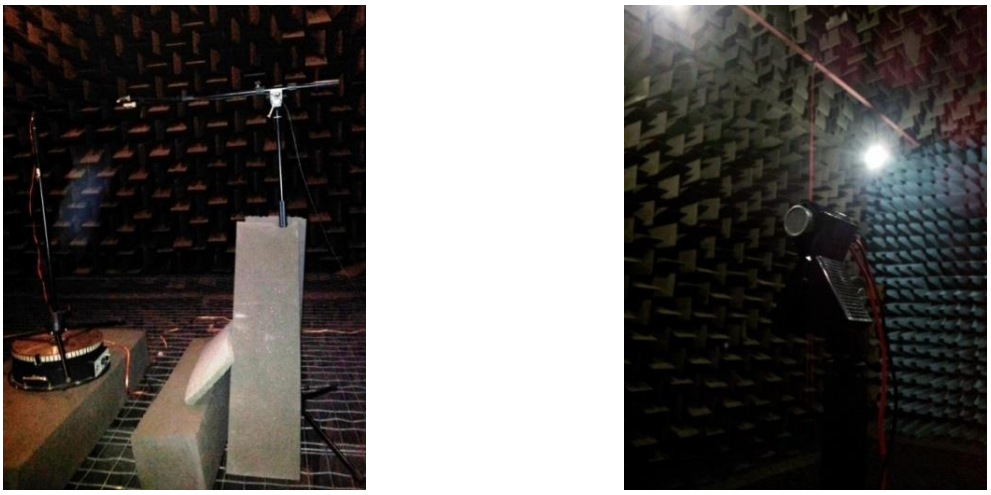

(a) (b)

Figure 3.2. Experimental setup within the anechoic room. (a) Microphone stand covered with acoustic foam (right) and ultrasound transducer (left) set on a microphone stand located on the turntable. (b) Detail of an ultrasound transducer and the microphone clip.

The generated sound pressure was then measured up to 80 kHz with a free-field microphone of ¼ inch (G.R.A.S. 40BF) and recorded with the acquisition card through a Nexus conditioning amplifier. The recorded signal included the audible sound level, ultrasonic side band level and the carrier level. By means of a turntable B&K 9640, the transducers were tested from zero degrees to ninety degrees in five degree increments in order to obtain directivity information. The microphone stand was covered with acoustic foam in order to minimize spurious reflections.

3.3 Measurement results

3.3.1 Pressure level at 1 kHz

The sound pressure level (SPL) was first measured when the transducer is driven with a sinusoidal signal of 1 kHz modulated with USBAM. In Table 3.1 the obtained ultrasonic SPL and that of the generated audible signal are listed for the transducers under test. In addition, the efficiency of each transducer is also reported, which stands for the pressure level difference between the generated audible sound and the necessary ultrasonic level to produce it.

Table 3.1. Sound pressure level in dB measured for a sinusoid of 1 kHz modulated with USBAM. "Sound 1 kHz" stands for the audible signal at 1 kHz, "Ultrasound 1 kHz" for the modulated sine tone located in the ultrasonic range, and "Efficiency 1 kHz" for the difference between both measures.

Transducer	Sound 1kHz	Ultrasound 1kHz	Efficiency 1kHz
Murata 10mm	60.65	113.30	-52.65
Multicomp 10mm	61.45	114.63	-53.18
Prowave 10mm	56.26	111.29	-55.03
Prowave 12mm	62.02	113.04	-51.02
Multicomp 16mm Transciever	70.26	121.05	-50.79
Multicomp 16mm Transmitter	69.06	117.44	-48.38
Prowave 16mm	70.96	119.38	-48.42

3.3.2 Frequency response

Figure 3.2 presents the frequency response measured at zero degrees for each ultrasound transducer in the audible (top) and ultrasonic (bottom) frequency ranges. Note that in the latter we only show the region corresponding to the upper side band where the sine tones are modulated.

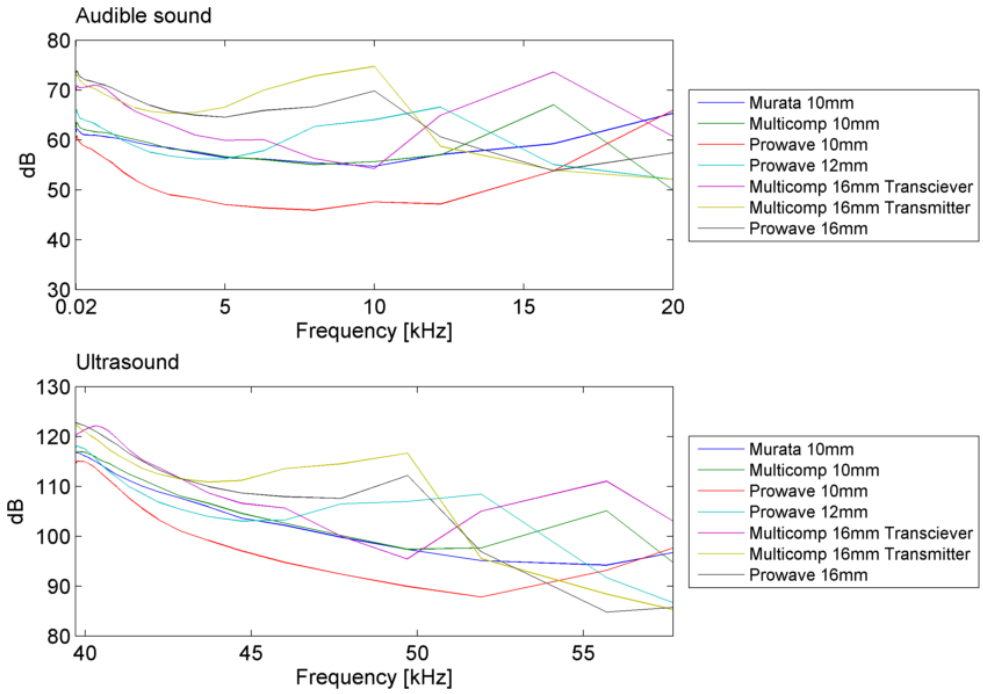

Figure 3.2. Frequency response at 0º for different ultrasound transducers measured at 30 cm. (Top) Produced audible sound and (bottom) generated ultrasound.

3.3.3 Directivity patterns

Figure 3.3 shows the obtained directivity patterns for each ultrasound transducer in the audible frequency range (top) and in the ultrasonic range (bottom) , where the sine tones are modulated. All directivity patterns are normalized with the SPL at 1 kHz (modulated 1 kHz for the ultrasound).

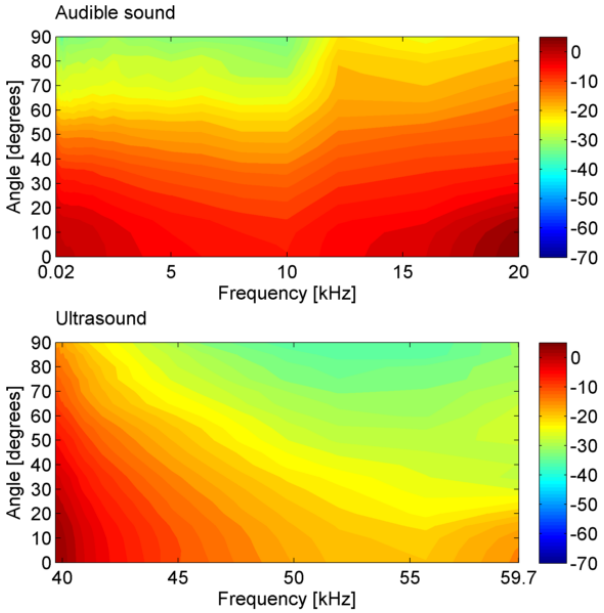

(a) Murata 10mm

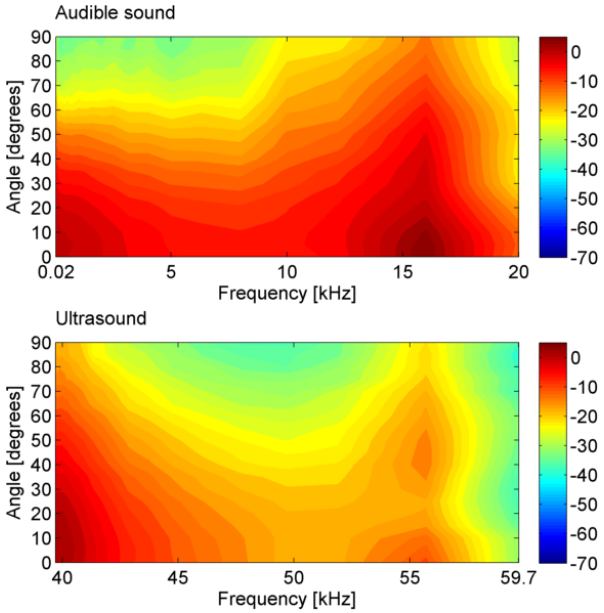

(b) Multicomp 10mm

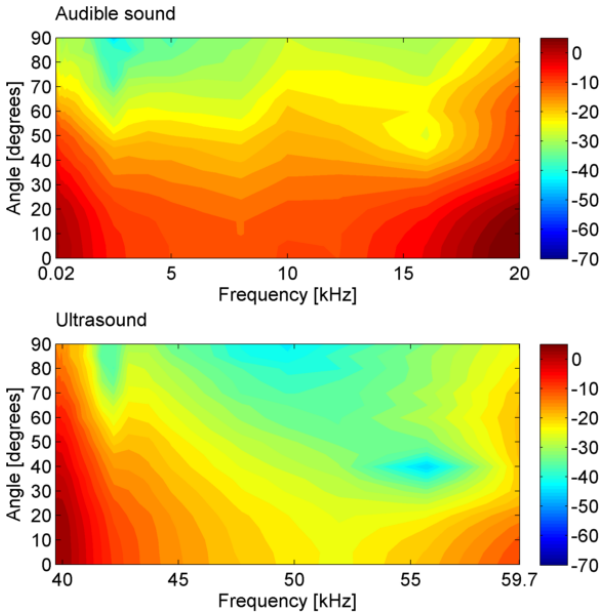

(c) Prowave 10mm

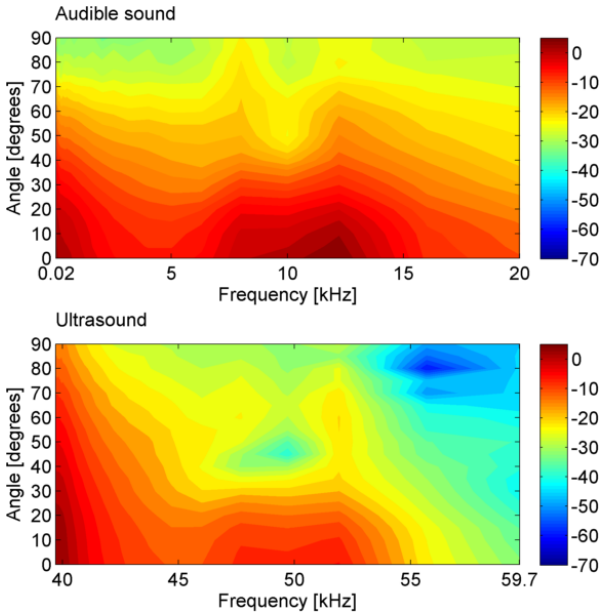

(d) Prowave 12mm

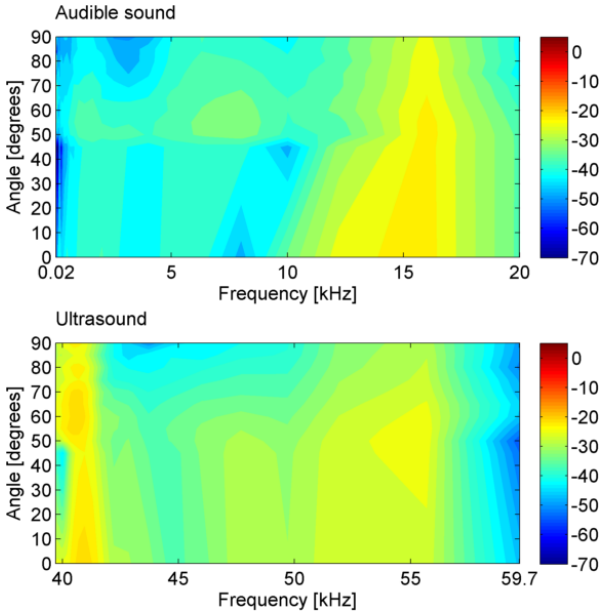

(e) Multicomp 16mm Transciever

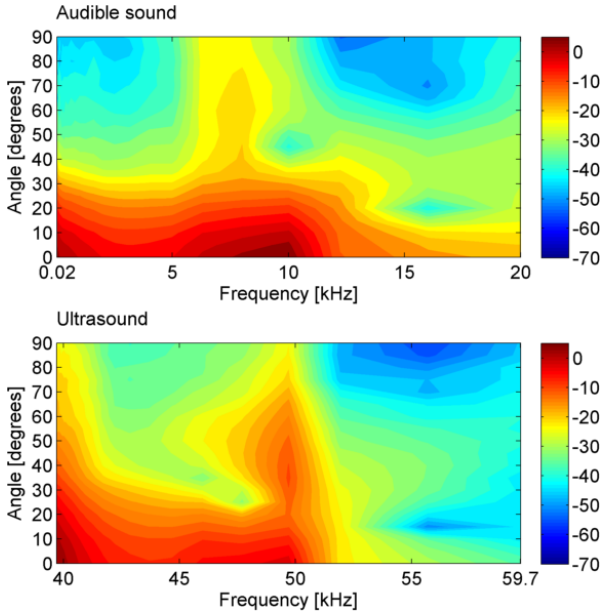

(f) Multicomp 16mm Transmitter

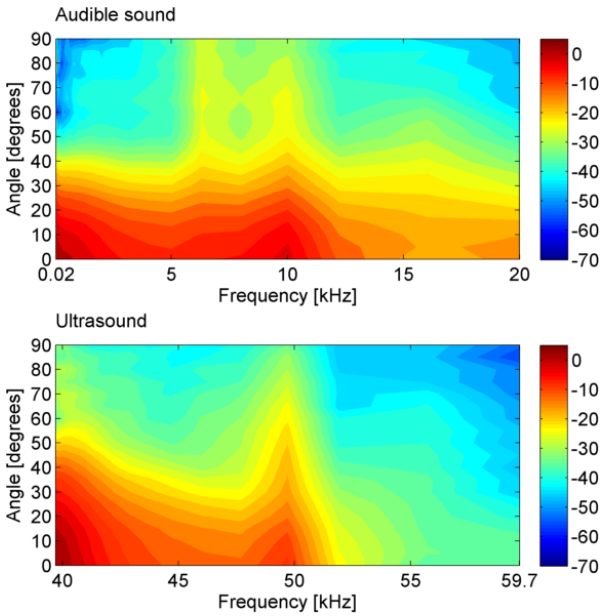

(g) Prowave 16mm

Figure 3.3. Directivity patterns for audible and ultrasonic sound pressure levels for different transducers. All directivity patterns are normalized with the sound pressure level at 1 kHz (or the equivalent modulated 1 kHz for the ultrasonic sound).

3.3.4 Carrier level

Figure 3.4 presents the sound pressure level of the carrier for every transducer when the different test signals are introduced.

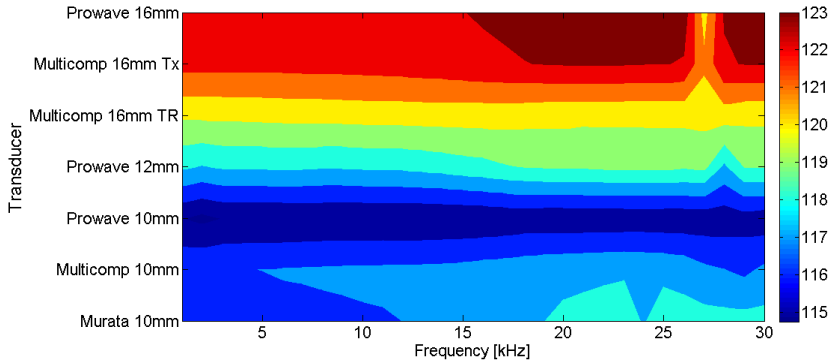

Figure 3.4. Variation of carrier sound pressure level with emitting signals of different frequencies. The *x*-axis represents the frequency range while the *y*-axis represents the transducer model.

3.4 Conclusions

As expected, the smaller transducers have shown minor levels of audible and ultrasonic sound pressure levels (SPL) than the larger ones due to smaller piezo component. They have also provided a wider coverage due to less directive nature. In general, all the transducers have shown a relatively flat frequency response in the audible frequency range. This is due to the 12 dB increase per octave in audible SPL in the secondary field which becomes compensated by the resonant nature of the transducer. In what concerns the carrier level, it can be considered constant throughout the frequency range. Thus, the most important component to define the amount of audible SPL is the upper side band component. The calculated variation for the carrier level did not surpass 1dB in the majority of the transducers with the exception of "Prowave 16mm" which had a variation of 1.5dB.

In view of the results, the "Multicomp 16mm transmitter" seems to be the best candidate for building the first OPL prototype (OPL#1). It provides high SPLs for both the audible and ultrasound ranges, and also one of the best efficiencies. Moreover, it gives loud SPLs at low frequencies, a range where this technology typically has more difficulties. Compared to smaller transducers, less transducers are needed to build an OPL, henceforth reducing the costs, yet this also means that a smaller amount of transducers will contribute to the total SPL of the OPL. The "Multicomp 16mm transmitter also has a more directive behaviour which may pose some difficulties to reach an omnidirectional directivity pattern in the OPL, but this could be circumvented with a high density of transducers over the sphere surface.

4 Characterization of the OPL#1

4.1 Introduction

The OPL#1 was built using the ultrasound transducer "Multicomp 16mm transmitter", but with an aluminium cover. The OPL diameter was 0.2 m and a total of 255 transducers were used (see Figure 4.1). Details of the construction and design can be found in "D3.10 Parametric loudspeaker prototypes".

Figure 4.1. OPL#1 prototype set on a microphone stand.

The OPL#1 was tested in laboratory conditions with different types of measures and sound test signals. These include measurements of the frequency response, sound pressure levels (SPL) and directivity in an anechoic chamber, and SPL and diffusion measurements in a reverberant chamber.

4.2 Measurement description

The following measurements have been performed:

- **Frequency response:** the performance of the OPL#1 was evaluated using white noise and sine sweeps. Measurements were performed at 1 meter of distance.

- **SPL in an anechoic chamber:** three types of sound test signals were used to measure the SPL in third-octave bands that the OPL#1 produces. These consisted of pure tones with third-octave central frequencies, broadband white noise, and a sine sweep signal. Measurements were performed at 1 meter of distance for the OPL#1 prototype. Measurements for the ultrasound transducer "Multicomp 16mm" were also performed under the same conditions to facilitate comparison with the OPL.

- **Directivity:** pure tones with third-octave central frequencies from 125Hz to 8 kHz were used to evaluate the directivity of the OPL#1. Measurements were performed at 1 meter of distance.

- **SPL in a reverberant chamber:** sine sweeps were used to measure the SPLs in a diffuse field. 20 measurements were performed locating the OPL and the microphone randomly within a reverberant chamber. The SPL in third-octave bands is provided by averaging all the SPLs of each measurement.

- **Diffusion:** the diffusion of a reverberant chamber was evaluated using warble tones from 100 Hz to 20 kHz.

4.3 Experimental setup

4.3.1 Frequency response

The frequency response of the OPL#1 prototype was measured within the anechoic chamber of La Salle, Universitat Ramon Llull (see Figure 4.2). Moreover, for comparison purposes, the Multicomp16mm ultrasound transducer used for the construction of this prototype was also characterized under the same conditions.

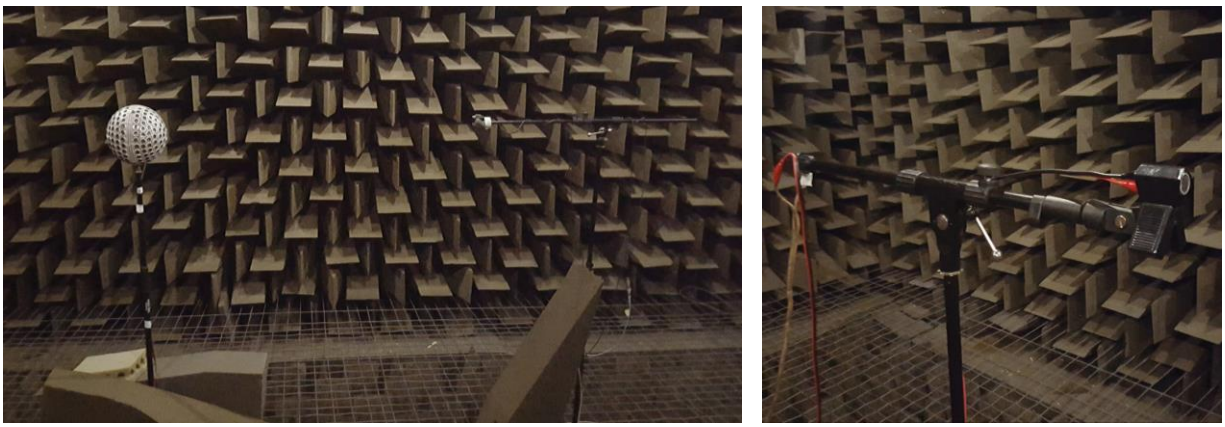

(a) (b)

Figure 4.2. Experimental setup within the anechoic chamber for measuring the frequency response of (a) the OPL#1 prototype and the (b) Multicomp16mm ultrasound transducer. In (b) a detail of the ultrasound transducer is shown.

A swept-sine technique was used to measure the impulse response. In particular, the following exponential sine sweep was generated

$$x(t) = \sin\left[K\left(e^{t/L} - 1\right)\right] K\,, \tag{4.1}$$

with

$$K = \frac{2\,\pi\ f_1\,T}{\ln(f_2/f_1)}\ , L = \frac{T}{\ln(f_2/f_1)}, \tag{4.2}$$

and f_1 and f_2 respectively denoting the lower and higher frequencies in Hz of the measurement. T is the time duration in seconds. Note that the instantaneous frequency of $x(t)$ sweeps slowly at low frequencies and faster at higher ones, which results in a pink spectrum. A flat white spectrum would be obtained with a linearly-swept sine signal.

The sine sweep in (4.1) was generated with $f_1 = 20$ Hz and $f_2 = 24$ kHz to cover the whole audible range, and $T = 14$ s to ensure a good signal to noise ratio. A linear fade-in from 20 Hz to 80 Hz and a linear fade-out from 20 kHz to 24 kHz were applied to the global signal to reduce the pre-ringing artefacts of the measured impulse response. Moreover, 2 seconds of silence were added at the end of the signal to ensure that the direct sound reaches the microphone.

The swept-sine signal was then modulated with USBAM and emitted trough a Data Translation 9832 card. This signal was amplified using an Ecler XPA3000 with an input voltage of 16 V_{rms}. This value was selected to avoid to damage the OPL#1, as it is clearly below the maximum voltage of 20 V_{rms} that the ultrasound transducers can tolerate. The generated sound pressure levels were measured with a free field microphone ¼ inch (G.R.A.S. 40BF) and recorded with the acquisition card through a Nexus conditioning amplifier. The microphone was located at 1 meter distance from the OPL#1 prototype and from the ultrasound transducer. Both were at a zero degree configuration.

The impulse response $h(t)$ was then computed by convolving the recorded swept-sine signal $y(t)$ with an inverse filter $f(t)$

$$h(t) = y(t) * f(t) \ , \tag{4.3}$$

where

$$f(t) = x(T - t)(f_2/f_1)^{-t/T} \ . \tag{4.4}$$

Note that $f(t)$ in (4.4) corresponds to the sine sweep in (4.1) reversed in time and multiplied by a modulation factor that compensates the pink spectrum of (4.1). The frequency response was then easily computed from (4.3) using the Fast Fourier Transform.

4.3.2 Directivity

The directivity of the OPL#1 prototype was also measured in the anechoic chamber of La Salle, Universitat Ramon Llull (see Figure 4.3). Pure tones with octave central frequencies from 125 Hz to 8 kHz were modulated with USBAM and emitted as test signals trough a Data Translation 9832 card. These signals were next amplified with an Ecler XPA3000 with an input voltage of 16 V_{rms}.

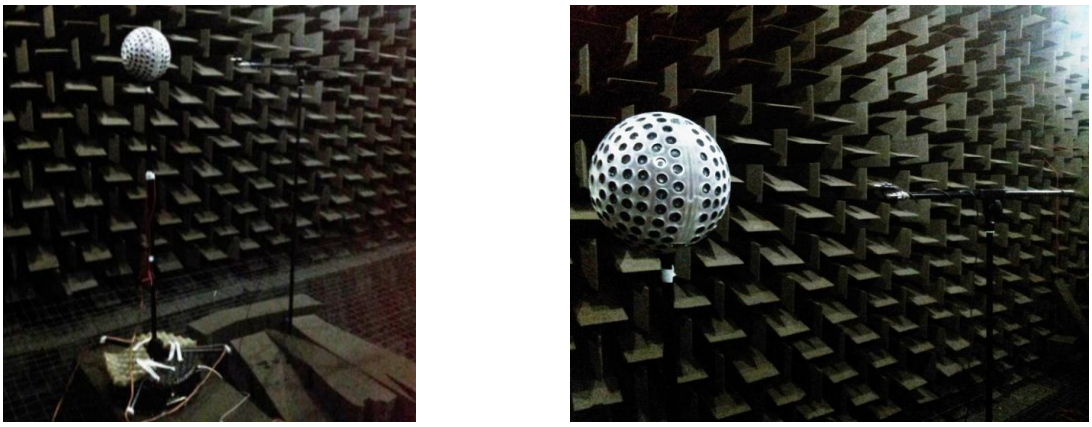

(a) (b)

Figure 4.3. Experimental setup within the anechoic chamber. (a) Microphone stand covered with acoustic foam (right) and OPL#1 prototype (left) set on a microphone stand located on the turntable. (b) Detail of OPL#1 and the microphone.

The OPL#1 rotates continuously from 0º to 360º by means of a turntable. The generated sound pressure levels were measured with a free field microphone ¼ inch (G.R.A.S. 40BF) for each degree and recorded with the acquisition card through a Nexus conditioning amplifier. The microphone was located at 1 meter distance.

4.3.3 Sound Pressure Levels in an anechoic chamber

The Sound Pressure Levels (SPL) of the OPL#1 prototype and the Multicomp16mm ultrasound transducer were measured at 1 meter distance within the anechoic chamber of La Salle, Universitat Ramon Llull (see Figure 4.2). These were computed in 1/3 octave-bands, typically used in acoustic measurements in buildings. Three types of test signals were examined:

- Pure tones with third octave central frequencies from 20 Hz to 20 kHz.
- An exponential swept-sine signal from 20 Hz to 24 kHz with 12 s of duration (see Section 4.3.1).
- White noise from 20 Hz to 20 kHz.

The experimental setup was similar to that described in Section 4.3.1 for measuring the frequency response. In the case of pure tones, the measured level for each tone directly corresponds to the energy of each one of the 1/3 octave-bands, as their frequencies were selected to be those of the central 1/3 octave-bands. For the swept-sine signal, the SPL in 1/3 octave-bands was computed from the frequency response measured in Section 4.3.1. This was done by energetically summing the frequency response levels that belong to each 1/3 octave-band, that is, from the lower to the upper limit of each band. A similar procedure was done for the white noise, but the levels were directly extracted from the spectrum of the recorded signal.

4.3.4 Sound Pressure Levels in a reverberant chamber

The Sound Pressure Levels (SPL) of the OPL#1 were also measured in the reverberant chamber of La Salle, Universitat Ramon Llull (Figure 4.4). Two types of tests signals were used:

- Pure tones with third octave central frequencies from 20 Hz to 20 kHz.
- An exponential swept-sine signal from 20 Hz to 24 kHz with 12 s of duration (see Section 4.3.1).

A set of 20 measurements were performed for each test signal. These consisted of 2 locations of the sound source combined with 5 positions for the microphone stand, and 2 repetitions for each pair of sound source and microphone. The SPLs in 1/3 octave-bands for each configuration were computed following a similar procedure than that described in the previous Section 4.3.3. The mean SPL within the reverberant chamber was finally computed as the energetic average of all measurements,

$$\mathrm{SPL}_{\mathrm{mean}} = 10\log\left(\frac{\sum_{i=1}^{N} 10^{dB_i/10}}{N}\right), \tag{4.5}$$

where dB_i stands for the SPL of the i-th measurement and N for the total number of measurements.

4.3.5 Diffusion

The diffusion of the reverberant chamber of La Salle, Universitat Ramon Llull (see Figure 4.3), was measured using the OPL#1, and also with a CESVA standard omnidirectional sound source for comparison purposes. Warble tones with third octave central frequencies from 100 Hz to 5 kHz were employed. The modulation bandwidth was set to 10% and the rate to 7 cycles/s. These warble tones were modulated with USBAM and emitted as test signals trough a Data Translation 9832 card. These signals were next amplified with an Ecler XPA3000 with an input voltage of 16 V_{rms}.

Figure 4.4. Experimental setup within the reverberant chamber. Two pairs of microphones and sound sources (OPL#1 and CESVA) distributed randomly in the chamber.

The generated sound field was measured with two pairs of ½ inch diffuse field microphones (G.R.A.S. 46AQ). For each pair of microphones, one of them was fixed while the other was displaced on axis from 0 cm to 20 cm with and increment of 4 cm.

The diffusion of the reverberant chamber was evaluated by computing the cross correlation coefficient

$$\rho(x_1,t_1,x_2,t_2)=\frac{E\{p(x_1,t_1)p(x_2,t_2)\}}{\sqrt{E\{p^2(x_1,t_1)\}E\{p^2(x_2,t_2)\}}}, \quad (4.6)$$

considering $t1=t2$. In Eq. (4.6), $p(x_1,t_1)$ and $p(x_2,t_2)$ respectively stand for the acoustic pressure measured by microphone 1 and microphone 2.

4.4 Measurement results

4.4.1 Frequency response

The frequency response of the OPL#1 is shown in Figure 4.5 together with that of the Multicomp16mm ultrasound transducer.

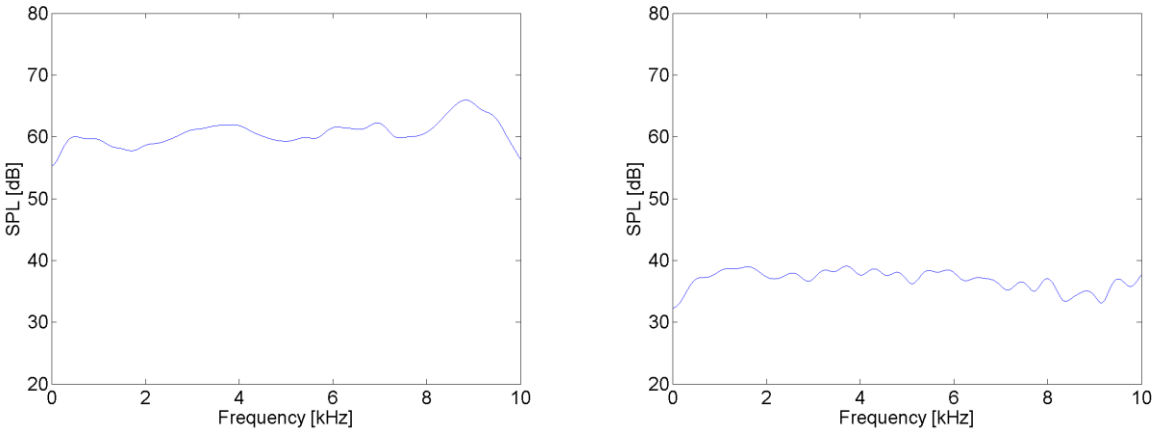

(b) OPL#1 (b) Transducer

Figure 4.5. Frequency response of the (a) OPL#1 and (b) the Multicomp16mm ultrasound transducer measured at 1 m with a swept-sine technique.

As it can be observed a quite flat acoustic response is obtained for the OPL#1 prototype in the examined frequency range. Moreover, as expected, the sound pressure levels have also increased with respect to the ultrasound transducer.

4.4.2 Directivity

Figure 4.6 shows the measured directivity patterns of the OPL#1 for each octave central frequency from 125 Hz to 8 kHz.

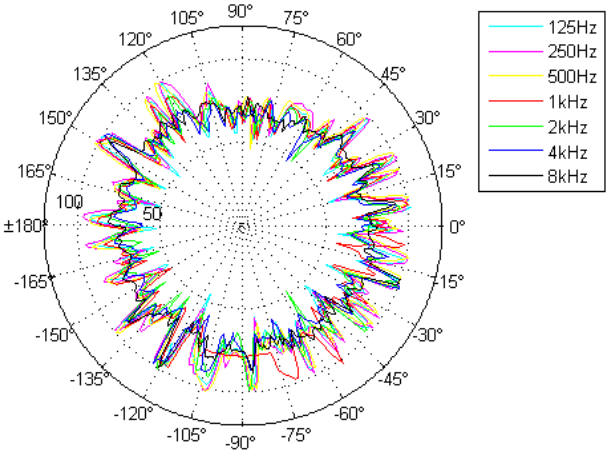

Figure 4.6. Directivity pattern of the OPL#1 at different frequencies.

As it can be observed in the figure, the OPL#1 radiates in all directions, but many sound pressure peaks and valleys are observed depending on the angle. This can be explained by looking at the location of the ultrasound transducers on the OPL#1 (see e.g. Figure 4.3b). Due to construction constrains (see D3.10), they were set too separated apart, thus producing higher pressure values when the microphone points to an ultrasound transducer and lower ones when it does not find any transducer. Moreover, the strip that joins the two hemispheres lacks of ultrasound transducers, so pressure levels clearly diminish in that area (see values at 90º and -90º). All in all, the directivity pattern of the OPL#1 clearly departs from the desired omnidirectional behaviour.

4.4.3 Sound Pressure Levels in an anechoic chamber

The sound pressure levels (SPL) in 1/3 octave bands generated by the OPL#1 prototype were measured at 1 meter distance under free-field conditions. Pure tones, sine sweeps and white noise were examined as test signals. For comparison purposes, the SPLs generated by a single Multicomp16mm ultrasound transducer, used for the construction of this prototype, were also measured under the same conditions.

Figure 4.7 presents the obtained results. The left column shows the SPLs for the OPL#1 and the right one those of the ultrasound transducer, while the top, middle and bottom rows respectively show the SPL values for the pure tones, sine sweep, and white noise. Results are expressed in dB_{SPL} for each 1/3 octave bands. Moreover, the total SPL is also provided, computed as the energetic addition of all the bands. All pressure values are summarized in Table 4.1.

Table 4.2. 1/3 octave-band sound pressure levels measured at 1 meter distance within the anechoic chamber for the OPL#1 prototype and the Mutlicomp16mm ultrasound transducer. Pure tones, an exponential sine sweep, and white noise are used as test signals. Values are expressed in dB_{SPL}.

1/3 octave-band (Hz)	OPL#1			Transducer		
	Pure tones	Sine sweep	White noise	Pure tones	Sine sweep	White noise
100	60.3	69.8	48.5	34.3	46.5	32.5
125	58.2	71.1	32.7	34.9	47.6	30.6
160	57.7	72.7	43.2	34.5	49.0	37.4
200	59.5	74.2	46.4	37.8	50.4	33.3
250	59.9	76.0	42.4	34.3	52.0	33.6
315	59.6	77.8	45.1	35.9	53.9	37.6
400	58.5	79.5	40.0	36.5	55.9	37.0
500	59.5	80.7	39.3	37.5	57.6	38.6
630	60.1	81.5	38.7	38.0	58.9	33.2
800	60.9	82.4	38.3	37.2	60.1	33.7
1000	59.1	83.2	39.2	38.4	61.9	35.0
1250	58.0	83.2	39.7	38.1	63.3	36.2
1600	56.7	83.6	40.2	40.4	64.5	36.3
2000	57.1	85.2	40.9	37.6	64.2	37.5
2500	59.1	87.3	42.2	37.0	65.2	38.5
3150	61.1	90.0	43.1	38.1	66.4	39.1
4000	62.6	91.1	44.4	37.4	68.1	39.2
5000	61.2	90.3	46.1	35.5	68.3	38.6
6300	62.8	93.0	45.7	36.5	69.0	38.4
8000	59.1	95.5	46.6	33.9	68.1	38.1
10000	56.2	96.4	49.2	34.8	71.2	38.5
Total	**73.0**	**101.9**	**57.3**	**50.1**	**77.9**	**50.2**

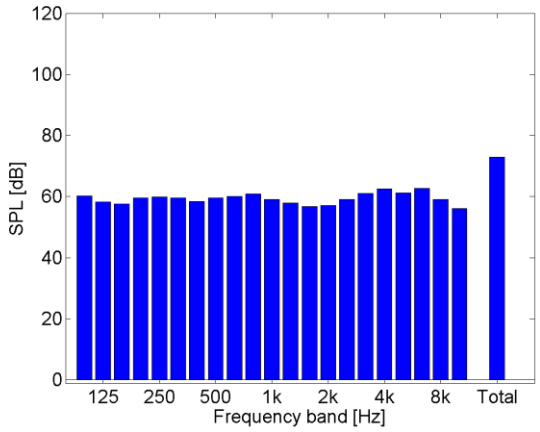

(a) OPL#1 – Pure tones

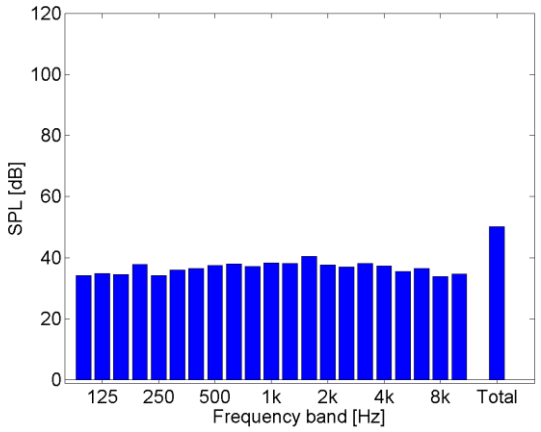

(b) Transducer – Pure tones

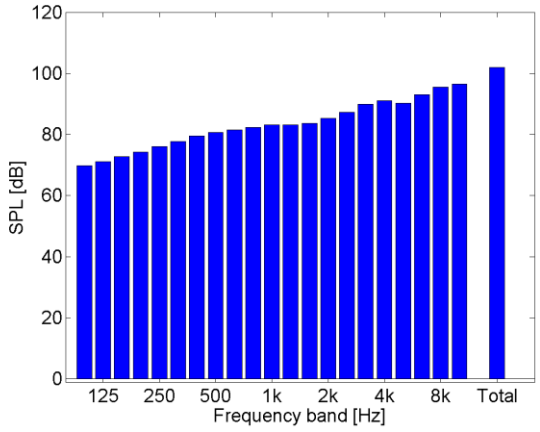

(c) OPL#1 – Sine sweep

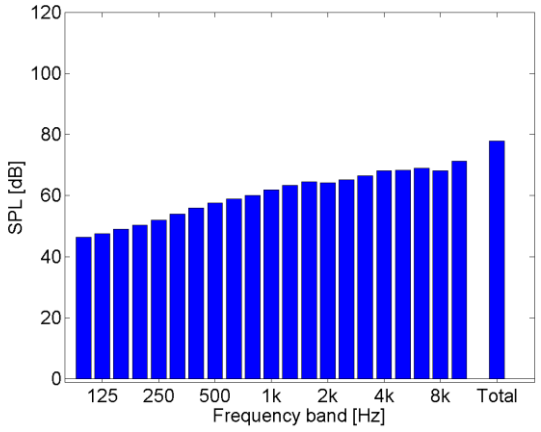

(d) Transducer – Sine sweep

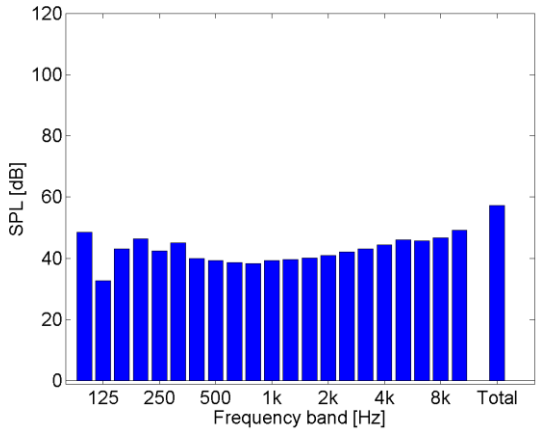

(e) OPL#1 – White noise

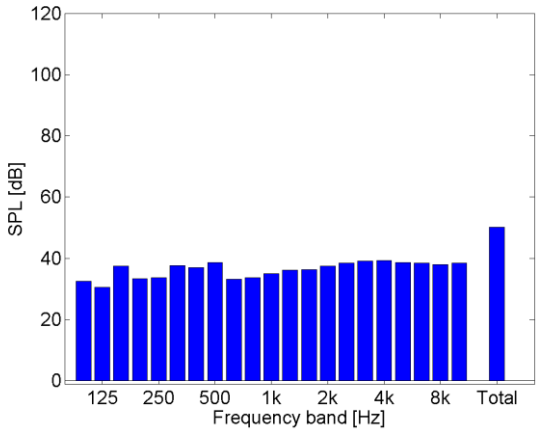

(f) Transducer – White noise

Figure 4.7. Sound Pressure Levels (SPL) in 1/3 octave-bands measured for (left) the OPL#1 and (right) the Mutlicomp16mm ultrasound transducer at 1 m distance within the anechoic chamber. Three kind of excitations were used: (top) pure tones, (middle) an exponential sine sweep, and (bottom) white noise.

As it can be observed, both in the Figure 4.7 and Table 4.1, the test signal that provides the highest SPLs is the sine sweep, the second one are the pure tones, and the third one is the white noise. This is so because using sine signals all the emitted power can be concentrated into a single frequency, in contrast to what occurs with the white noise, where the energy is spread in a wide frequency range. While this could be admissible for standard loudspeakers (which directly generate audible sound), this behaviour is more critical for the technology the OPL is based upon. Strong enough ultrasound pressure levels are not achieved when using white noise, so that the non-linearities of the air that demodulate this signal into the audible frequency range are not properly activated, thus reducing even more the generated audible levels compared to a standard loudspeaker. As far as the sweep signal is concerned, it obviously increases the sound pressure levels compared to the pure tones, as it contains all the frequencies for each 1/3 octave band.

Comparing the OPL with the ultrasound transducer, a significant increase of the SPL is obtained for all the test signals, with the exception of the white noise. This is so because for the latter signal the SPLs are close to the background noise, which limits the measurement to lower SPLs.

4.4.4 Sound Pressure Levels in a reverberant chamber

The mean SPL in 1/3 octave bands was also measured in a diffuse field, but this time only sine sweeps were used as excitation. Compared to the other test signals, sine sweeps showed to provide the highest SPL during the tests performed within the anechoic chamber (see Section 4.4.3). Figure 4.8 shows the obtained results for the OPL#1 and Table 4.2 contains all the SPL values in the figure. To facilitate comparison, the results obtained within the anechoic chamber (SPL at 1 meter) are also presented.

Table 4.2. Mean Sound Pressure Levels (SPL) in 1/3 octave-bands within the reverberant chamber for the OPL#1 prototype, and SPL measured at 1 meter within the anechoic chamber. An exponential sine sweep was used as test signal. Values are expressed in dB_{SPL}.

1/3 octave-band (Hz)	Mean SPL (reverberant chamber)	SPL @ 1m (anechoic chamber)	Differences (reverberant-anechoic)
100	54.7	69.8	-15.1
125	56.6	71.1	-14.5
160	59.1	72.7	-13.6
200	61.5	74.2	-12.7
250	64.3	76.0	-11.7
315	67.2	77.8	-10.6
400	70.1	79.5	-9.4
500	72.5	80.7	-8.2
630	74.5	81.5	-7
800	76.5	82.4	-5.9
1000	78.2	83.2	-5
1250	79.3	83.2	-3.9
1600	80.6	83.6	-3
2000	82.4	85.2	-2.8
2500	84.8	87.3	-2.5
3150	86.8	90.0	-3.2
4000	87.8	91.1	-3.3
5000	88.5	90.3	-1.8
6300	90	93.0	-3
8000	91.2	95.5	-4.3
10000	92.3	96.4	-4.1

Total	98.4	101.9	-3.5

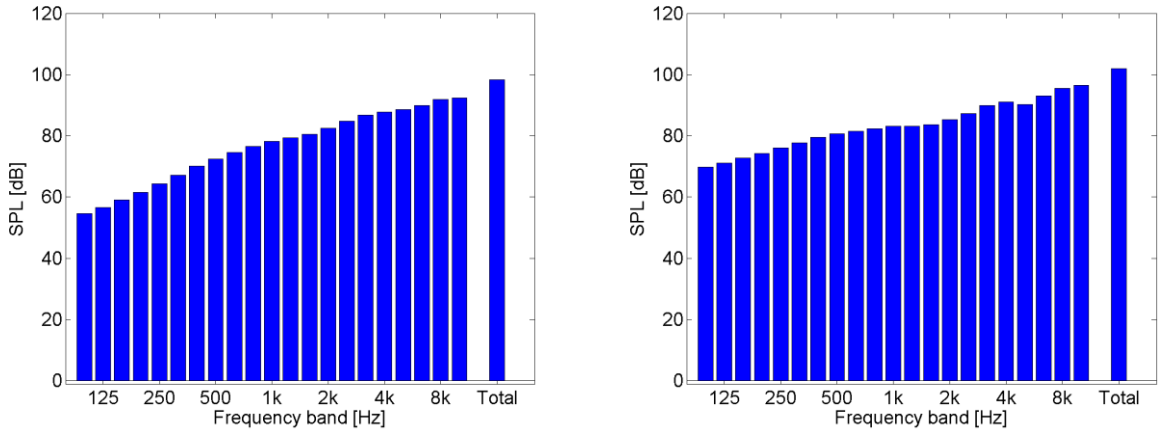

(a) Mean SPL within the reverberant chamber (b) SPL at 1 m within the anechoic chamber

Figure 4.8. (a) Mean Sound Pressure Levels (SPL) within the reverberant chamber in 1/3 octave-bands measured for the OPL#1, and (b) SPL at 1 meter within the anechoic chamber. An exponential sine sweep was used as test signal.

In terms of total SPL, the pressure values measured within the reverberant chamber have decreased by 3.5 dB compared to those measured within the anechoic chamber (see Table 4.1). Moreover, the spectral shape has also changed (see also Figure 4.8). While at high frequencies the differences are not really large, at low frequencies they increase significantly, obtaining deviations up to 15 dB.

One should keep in mind that the SPLs within the anechoic chamber were measured at 1 meter distance, and that they would be reduced if we increased the measurement distance. In contrast, the SPLs within the reverberant chamber come from the mean between 20 measurements, so they are independent of the microphone position in this sense.

However, some of the observed differences could be explained by the following reasons. On the one hand, the SPLs within the anechoic chamber are not very high. One could then hypothesize that the OPL#1 may not have enough acoustic power to excite the reverberant chamber. On the other hand, as shown in Section 4.4.2, the OPL#1 does not have an omnidirectional behaviour. In other words, not all the faces introduce the same acoustic power, which also influences the sound generation within the chamber.

4.4.5 Diffusion

The diffusion of the Reverberant chamber was evaluated by measuring the correlation coefficient with different two pairs of microphones. Figure 4.9 presents the obtained results when the OPL#1 and a standard omnidirectional loudspeaker (CESVA) are used as sound sources.

As it can be observed, lower values are obtained for the OPL#1 compared to the standard omnidirectional loudspeaker, which means that a more diffuse field is generated when using the OPL.

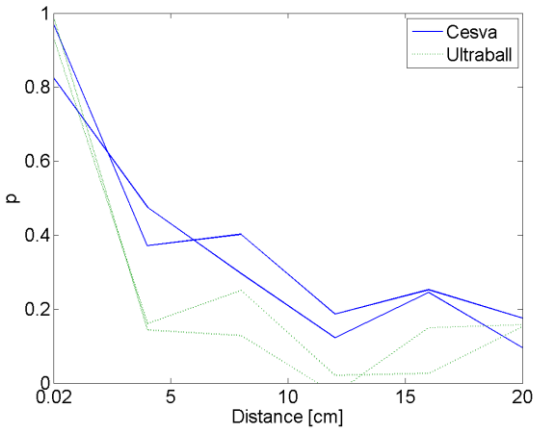

Figure 4.9. Cross correlation coefficient measured using two pairs of microphones. Continuous lines: standard omnidirectional loudspeaker (CESVA); dashed lines: OPL#1.

4.5 Conclusions

A quite flat frequency response has been obtained for the OPL#1 prototype in the examined frequency range. However, the directivity pattern was not as omnidirectional as one would desire, obtaining variations up to 20 dB depending on the angle and frequency. The SPLs generated by the OPL#1 have significantly been higher than those produced with a single transducer, with increments up to 27 dB depending on the frequency. Different test signals have been examined. These consisted of pure tones, an exponential sine sweep, and white noise. The exponential sine sweep has provided the highest SPL, as all the energy emitted by the OPL#1 can be concentrated in a single frequency. The total SPLs measured at 1 m within the anechoic chamber have reached a value of 101.9 dB, while within the reverberant chamber they have diminished to 98.4 dB. A better diffuse field has been obtained when comparing the correlation coefficient within the reverberant chamber with that of a standard omnidirectional loudspeaker.

All in all, the OPL#1 prototype has some issues that need to be fixed before it could be used for acoustic measurements. The most important one is that of the directivity pattern. We have then decided to build a second OPL prototype to fix this issue, which is currently under construction.

5 Characterization of ultrasound transducers for the OPL#2

5.1 Introduction

A new campaign of measurements was required for the design of the second OPL prototype (OPL#2). As described in D3.10 "Parametric loudspeaker prototypes", the improved theoretical model needs as input accurate directivity measurements of the ultrasound transducers in order to predict the total audible SPL generated by an OPL. Previous directivity measurements described in Section 3 were performed from 0º to 90º with 5º steps. More accurate measurements have then been performed from 0º to 360º with a continuously rotating turn table, obtaining an accuracy of 1º. In this occasion a smaller number of transducers have been tested. These are listed in what follows:

- **Murata 10mm (MA40S4S):** transmitter with a 10mm diaphragm. Plastic cover.
- **Multicomp 10mm (ST100):** transmitter with a 10mm diaphragm. Plastic cover.
- **Multicomp 16mm Transmitter (ST160):** transmitter with a 16mm diaphragm. Aluminum cover.

5.2 Experimental setup

The transducers were tested in the anechoic room of La Salle, Universitat Ramon Llull (see Figure 1).

The input signals were sinusoids corresponding to the octave band center frequencies from 125 Hz to 8 kHz. These sinusoidal signals were modulated with USBAM and emitted trough a Data Translation 9832 card. These signals were next amplified with an Ecler XPA3000 using two input voltages: 19.75 V_{rms} and 16 V_{rms}. These two values have been selected so as to avoid the maximum voltage of 20 V_{rms} that the ultrasound transducers can tolerate, and to test the variance in the directivity and SPL depending on the input voltage of the transducer.

By means of a turntable B&K 9640, the transducer rotate from 0º to 360º. The generated sound pressure was measured up to 80 kHz with a free field microphone ¼ inch (G.R.A.S. 40BF) for each degree and recorded with the acquisition card through a Nexus conditioning amplifier. The microphone was located at 1 meter distance from the transducer. The microphone stand was covered with acoustic foam to minimize spurious reflections.

(a) (b)

Figure 5.1. Experimental setup within the anechoic chamber. (a) Microphone stand covered with acoustic foam and transducer set on a microphone stand located on the turntable. (b) Detail of the transducer.

The temperature and the humidity inside the anechoic chamber during the measurements are listed in Table 5.1.

Table 5.1. Values of temperature and humidity within the anechoic chamber during the directivity measurement of each transducer.

Transducer	Temperature	Humidity
Murata 10mm	21,5 ºC	67 %
Multicomp 10mm	21,5 ºC	67 %
Multicomp 16mm	21,3 ºC	67 %

5.3 Measurement results

In what follows the results obtained for each transducer are presented.

5.3.1 Murata 10mm Transmitter

Figure 5.2 presents the directivity pattern of the Murata 10mm Transmitter for two different input voltages, showing all the frequencies in a single plot. In Figure 5.3 each frequency is split in a separate plot to better examine the individual patterns. Figure 5.4 shows the directivity pattern of the measured ultrasound levels (carrier frequency + octave-band central frequency).

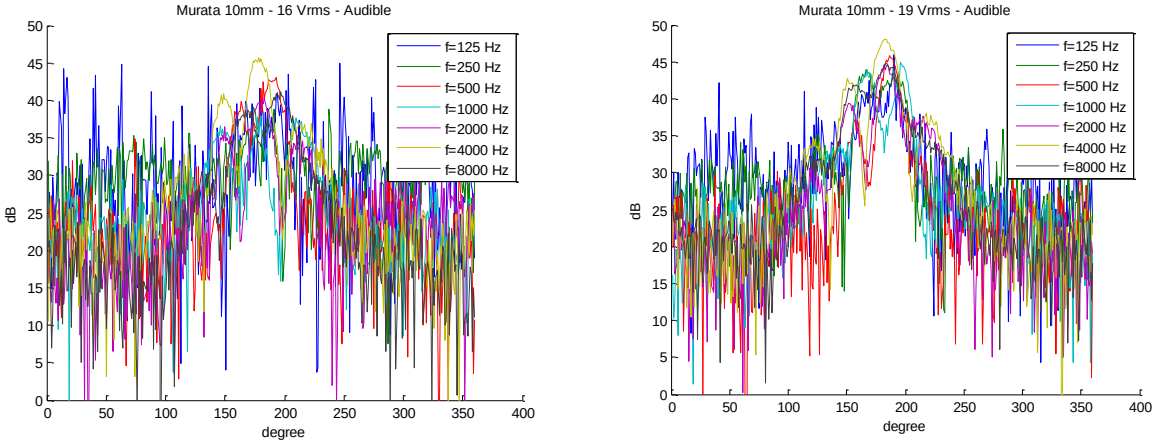

(a) 16 V_{rms} (b) 19.75 V_{rms}

Figure 5.2. Directivity pattern of the resulting audible signals when the Murata 10 mm transducer is used with an input voltage of (a) 16 V_{rms} and (b) 19.75 V_{rms}. Octave frequencies from 125 Hz to 8 kHz are overlapped.

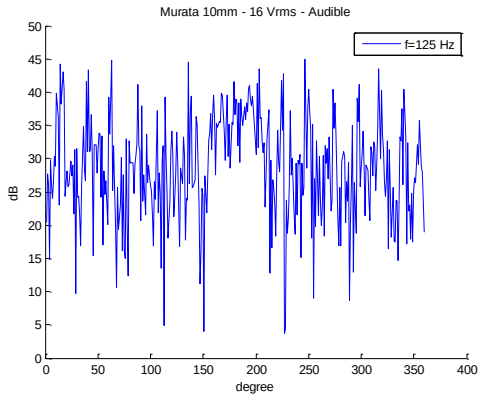

(a) 125 Hz – 16 V_{rms}

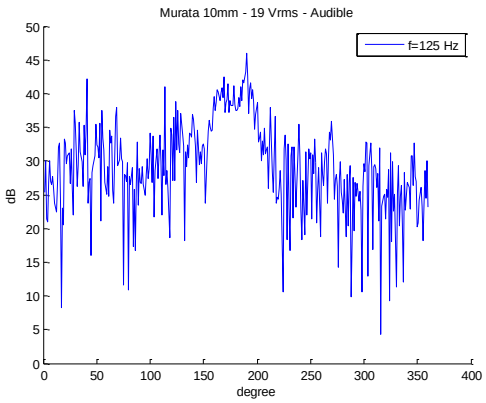

(b) 125 Hz – 19.75 V_{rms}

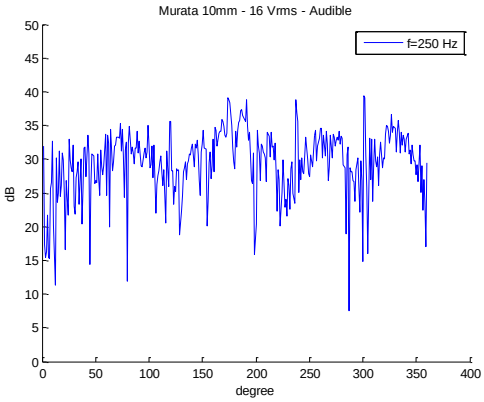

(c) 250 Hz – 16 V_{rms}

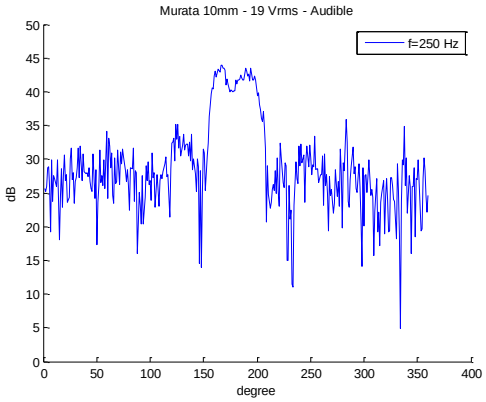

(d) 250 Hz – 19.75 V_{rms}

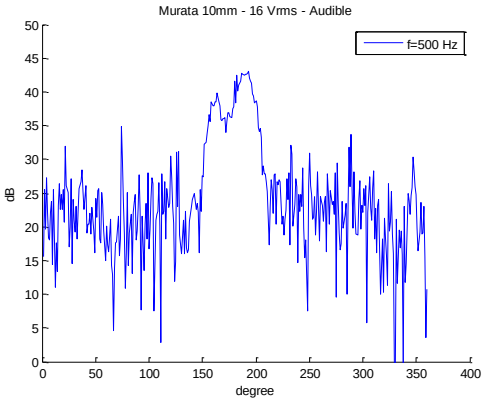

(e) 500 Hz – 16 V_{rms}

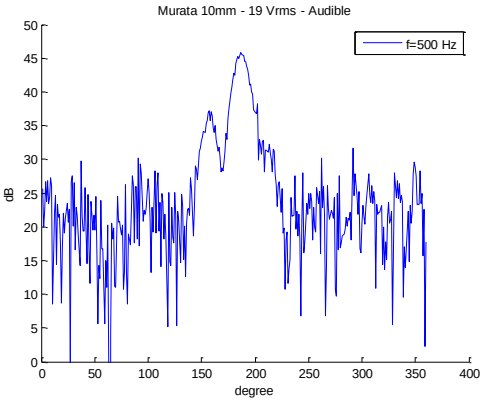

(f) 500 Hz – 19.75 V_{rms}

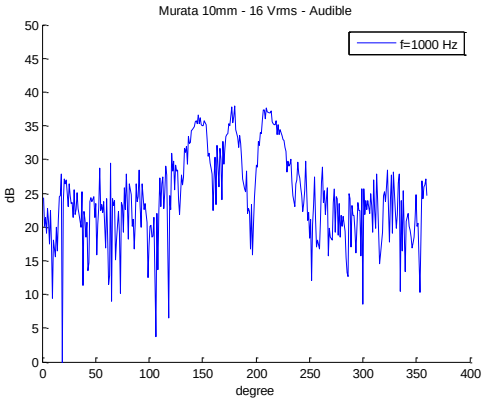

(g) 1 kHz – 16 V_{rms}

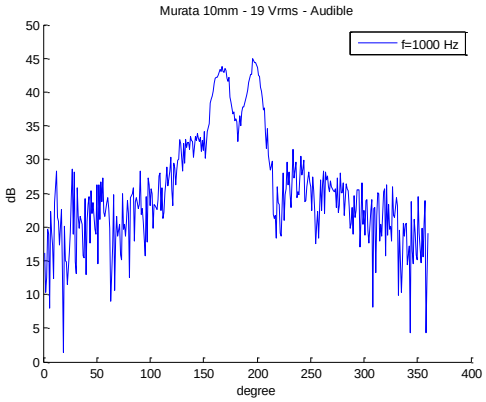

(h) 1 kHz – 19.75 V_{rms}

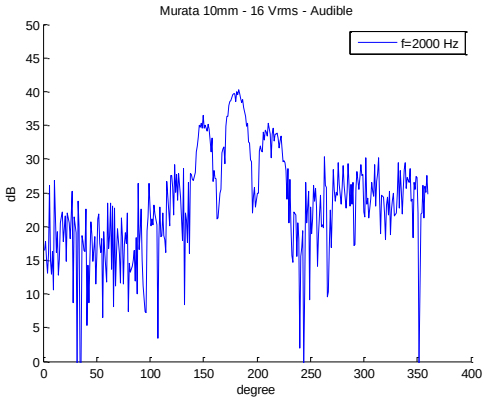

(i) 2 kHz – 16 V_{rms}

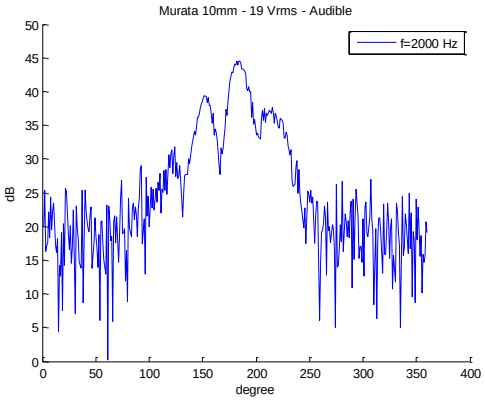

(j) 2 kHz – 19.75 V_{rms}

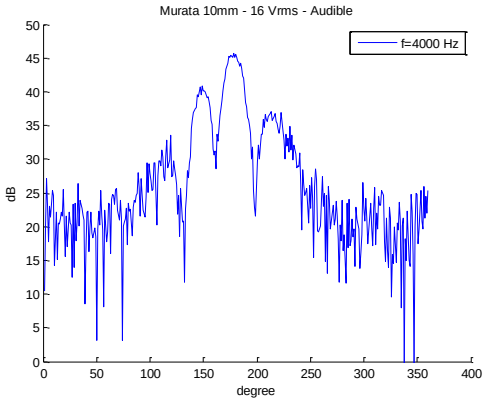

(k) 4 kHz – 16 V_{rms}

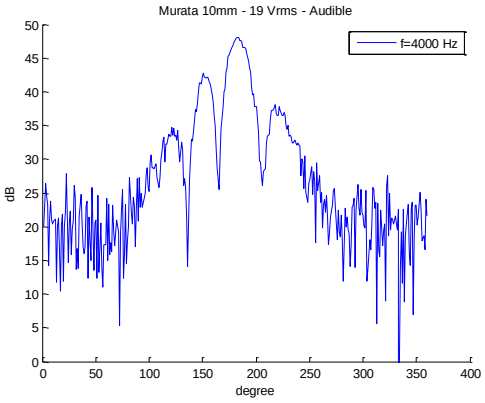

(l) 4 kHz – 19.75 V_{rms}

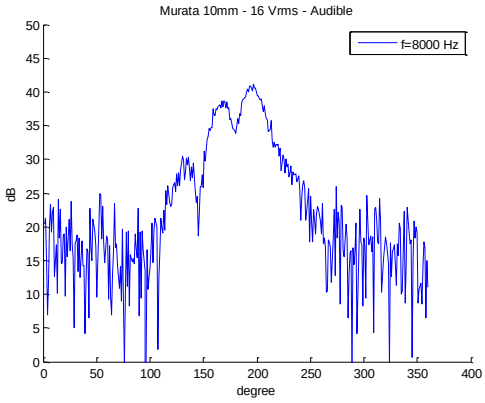

(m) 8 kHz – 16 V_{rms}

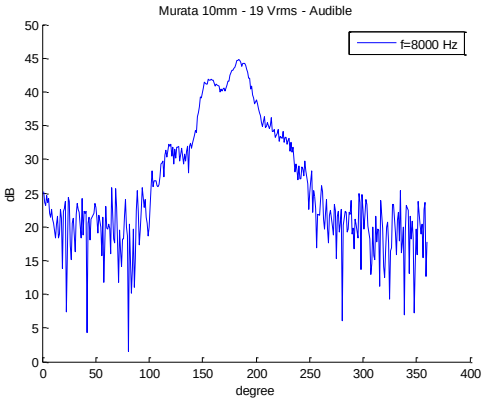

(n) 8 kHz – 19.75 V_{rms}

Figure 5.3. Directivity pattern of the resulting audible signals when the Murata 10 mm transducer is used with an input voltage of (a) 16 V_{rms} and (b) 19.75 V_{rms}. Octave frequencies from 125 Hz to 8 kHz are represented in independent figures.

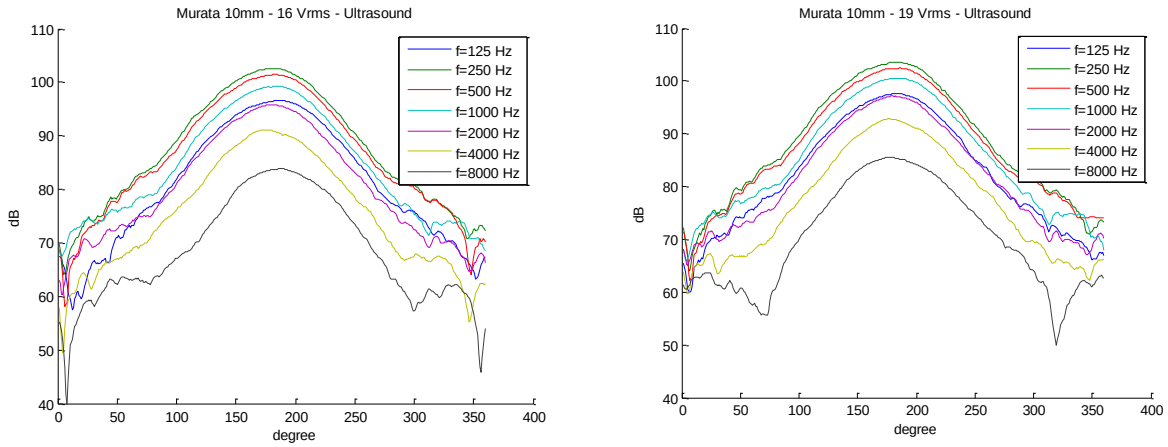

(a) 16 V_{rms} (b) 19.75 V_{rms}

Figure 5.4. Directivity pattern of the measured ultrasound levels (carrier frequency + octave-band central frequency) when the Murata 10 mm transducer is used with an input voltage of (a) 16 V_{rms} and (b) 19.75 V_{rms}. Octave frequencies from 125 Hz to 8 kHz are overlapped.

5.3.2 Multicomp 10mm Transmitter

Figure 5.5 presents the directivity pattern of the Multicomp 10mm Transmitter for two different input voltages, showing all the frequencies in a single plot. In Figure 5.6 each frequency is split in a separate plot to better examine the individual patterns. Figure 5.7 shows the directivity pattern of the measured ultrasound levels (carrier frequency + octave-band central frequency).

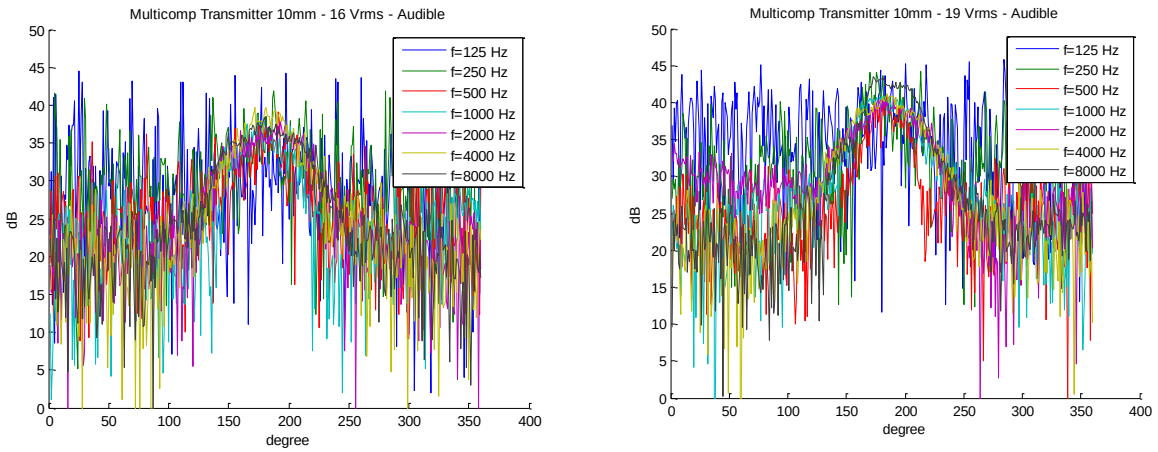

(a) 16 V_{rms} (b) 19.75 V_{rms}

Figure 5.5. Directivity pattern of the resulting audible signals when the Multicomp 10mm transducer is used with an input voltage of (a) 16 V_{rms} and (b) 19.75 V_{rms}. Octave frequencies from 125 Hz to 8 kHz are overlapped.

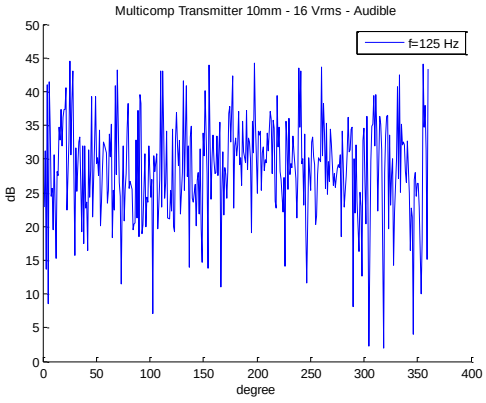

(a) 125 Hz – 16 V_{rms}

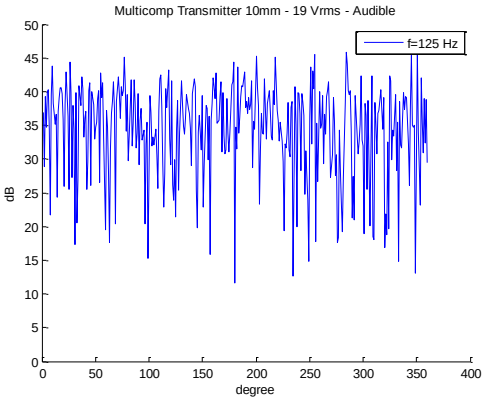

(b) 125 Hz – 19.75 V_{rms}

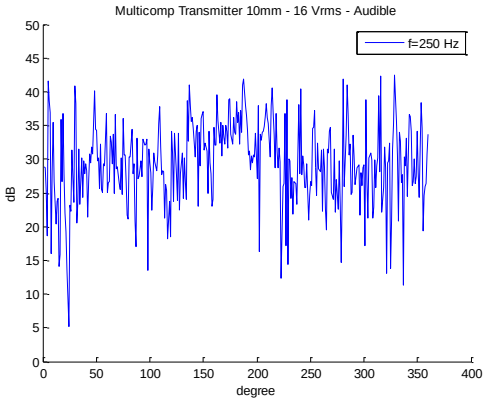

(c) 250 Hz – 16 V_{rms}

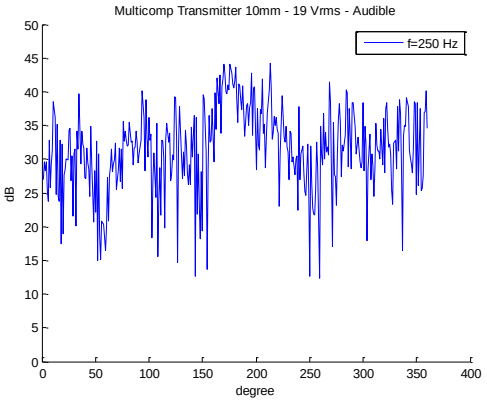

(d) 250 Hz – 19.75 V_{rms}

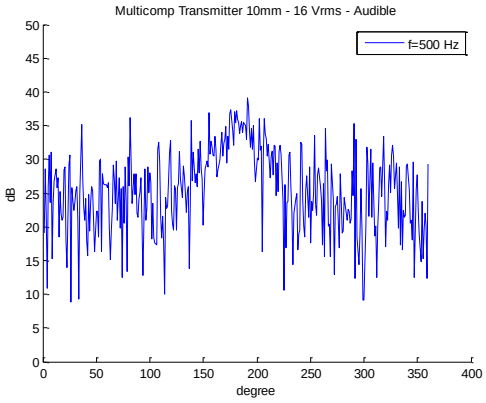

(e) 500 Hz – 16 V_{rms}

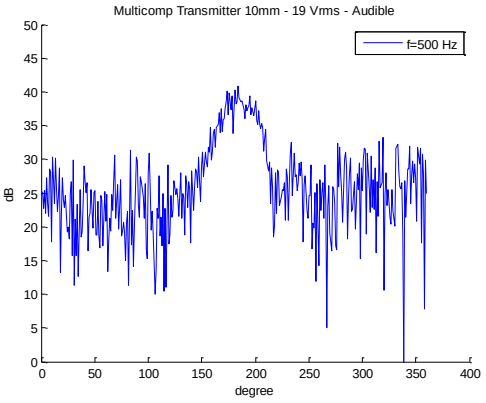

(f) 500 Hz – 19.75 V_{rms}

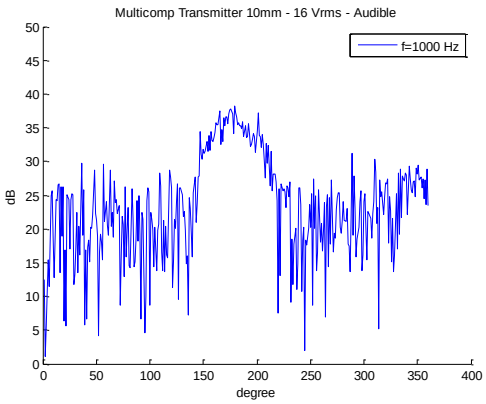

(g) 1 kHz – 16 V_{rms}

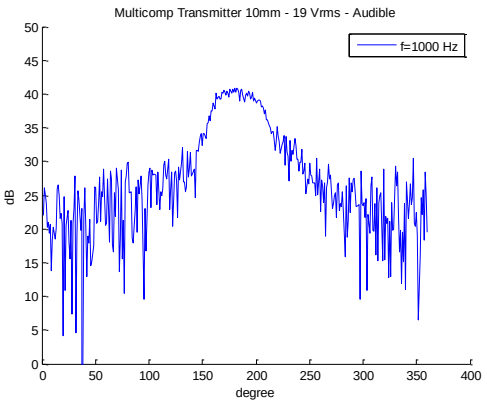

(h) 1 kHz – 19.75 V_{rms}

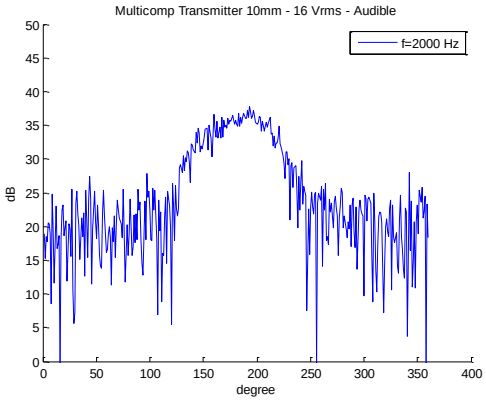

(i) 2 kHz – 16 V_{rms}

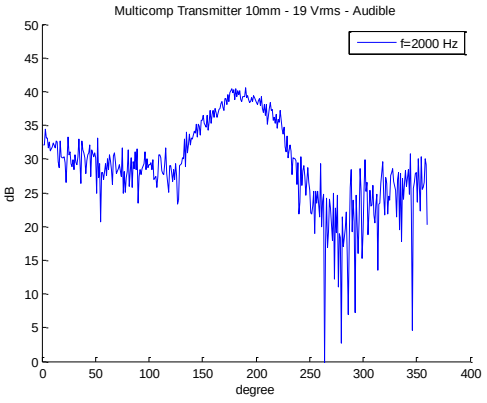

(j) 2 kHz – 19.75 V_{rms}

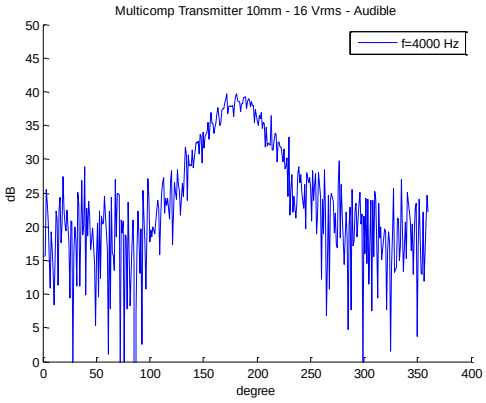

(k) 4 kHz – 16 V_{rms}

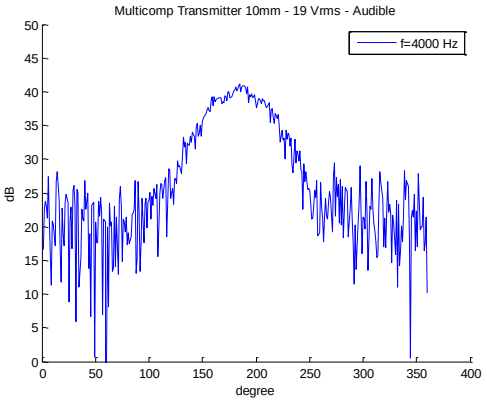

(l) 4 kHz – 19.75 V_{rms}

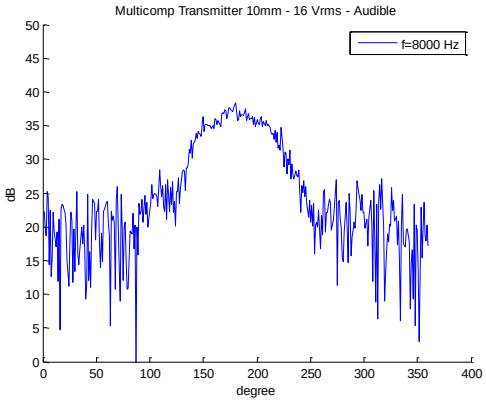

(m) 8 kHz – 16 V_{rms}

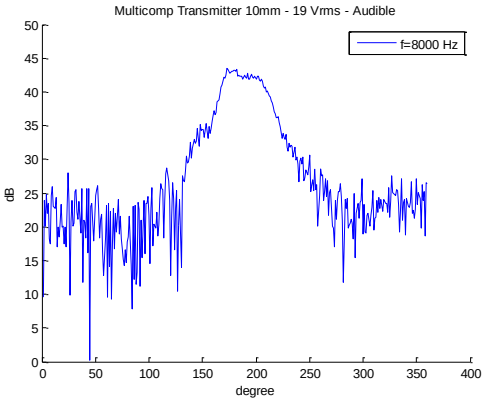

(n) 8 kHz – 19.75 V_{rms}

Figure 5.6. Directivity pattern of the resulting audible signals when the Multicomp 10mm transducer is used with an input voltage of (a) 16 V_{rms} and (b) 19.75 V_{rms}. Octave frequencies from 125 Hz to 8 kHz are represented in independent figures.

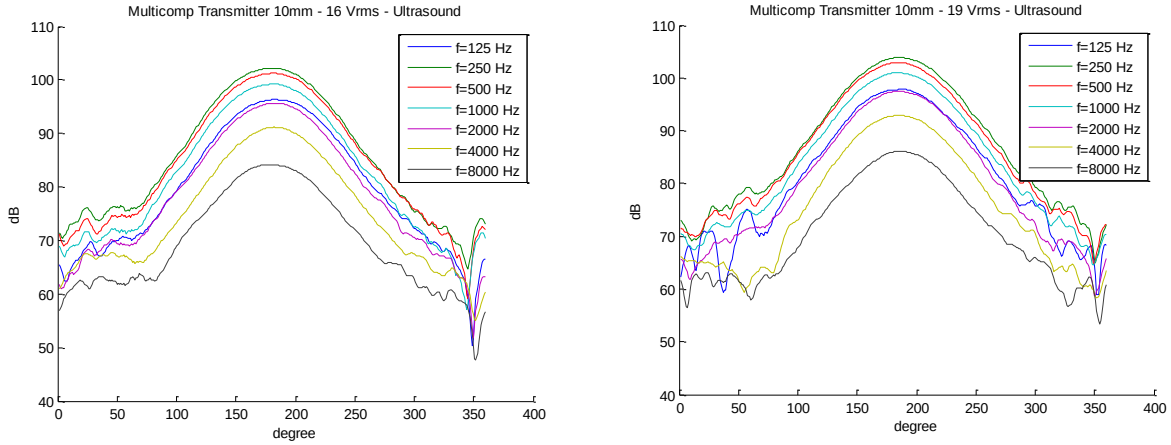

(a) 16 V_{rms} (b) 19.75 V_{rms}

Figure 5.7. Directivity pattern of the measured ultrasound levels (carrier frequency + octave-band central frequency) when the Multicomp 10mm transducer is used with an input voltage of (a) 16 V_{rms} and (b) 19.75 V_{rms}. Octave frequencies from 125 Hz to 8 kHz are overlapped.

5.3.3 Multicomp 16mm Transmitter

Figure 5.8 presents the directivity pattern of the Multicomp 16mm Transmitter for two different input voltages, showing all the frequencies in a single plot. In Figure 5.9 each frequency is split in a separate plot to better examine the individual patterns. Figure 5.10 shows the directivity pattern of the measured ultrasound levels (carrier frequency + octave-band central frequency).

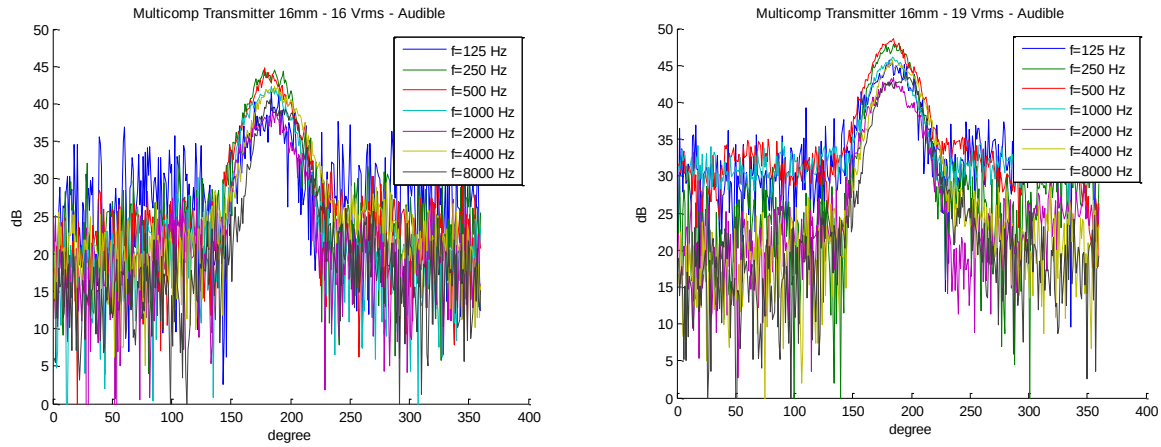

(a) 16 V_{rms} (b) 19.75 V_{rms}

Figure 5.8. Directivity pattern of the resulting audible signals when the Multicomp 16 mm transducer is used with an input voltage of (a) 16 V_{rms} and (b) 19.75 V_{rms}. Octave frequencies from 125 Hz to 8 kHz are overlapped.

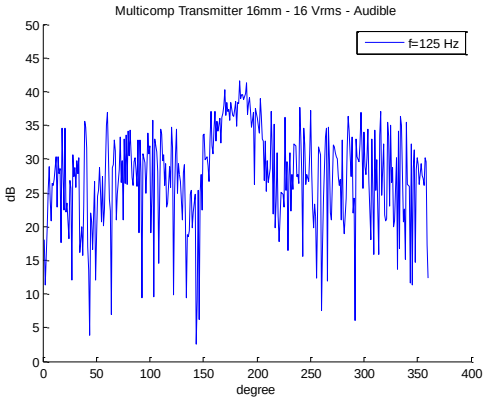

(a) 125 Hz – 16 V_{rms}

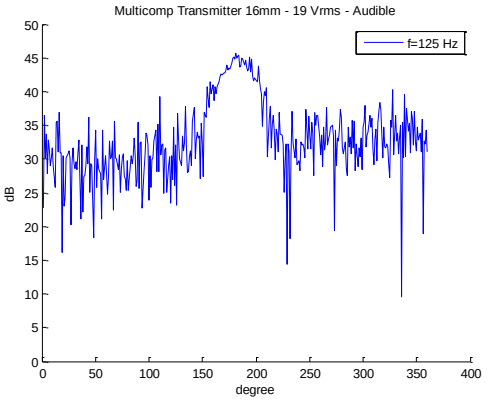

(b) 125 Hz – 19.75 V_{rms}

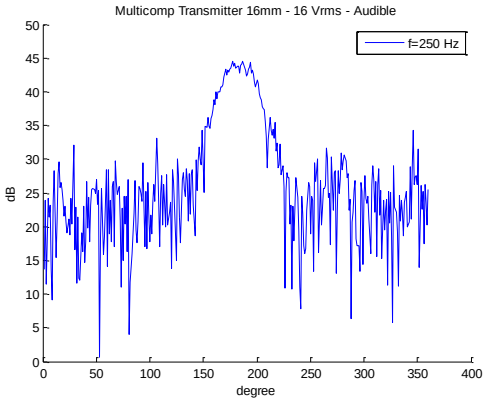

(c) 250 Hz – 16 V_{rms}

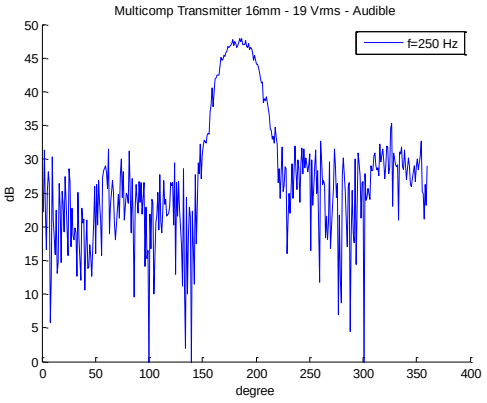

(d) 250 Hz – 19.75 V_{rms}

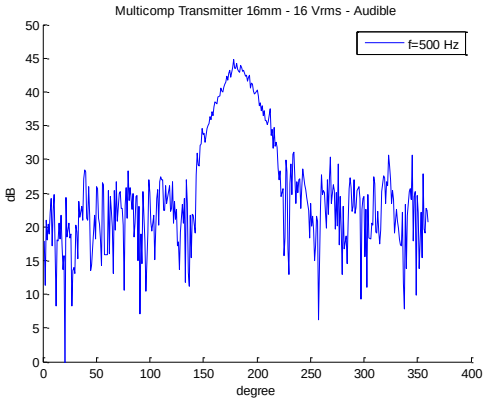

(e) 500 Hz – 16 V_{rms}

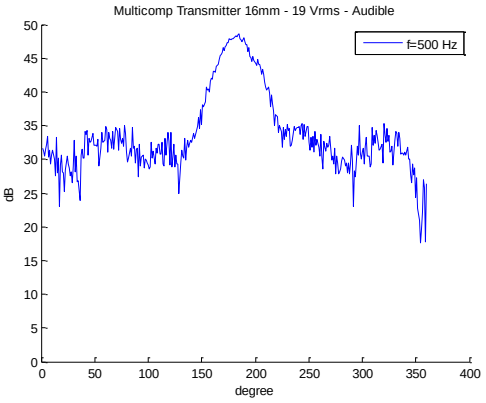

(f) 500 Hz – 19.75 V_{rms}

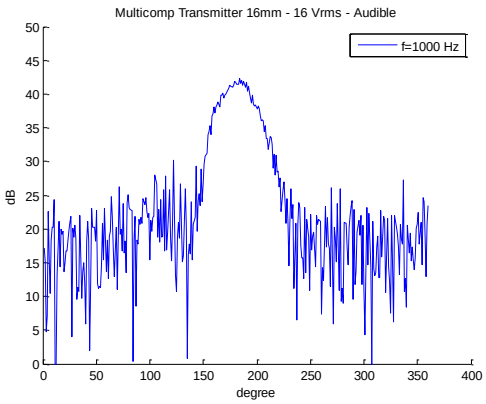

(g) 1 kHz – 16 V_{rms}

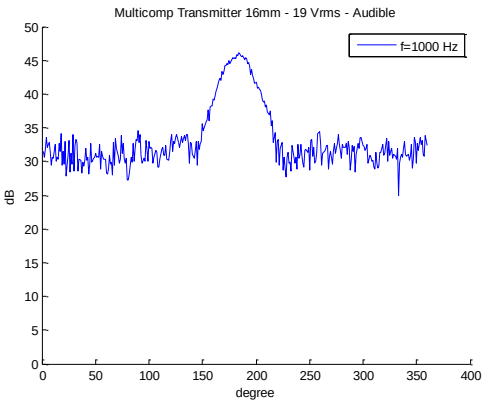

(h) 1 kHz – 19.75 V_{rms}

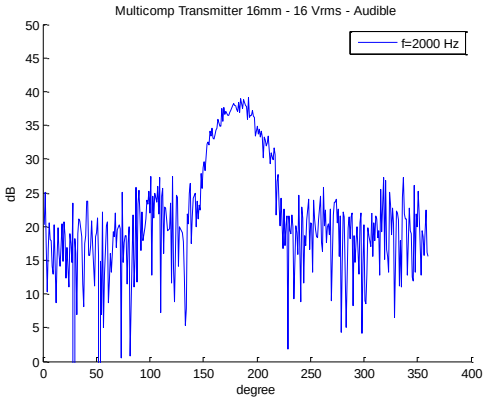

(i) 2 kHz – 16 V_{rms}

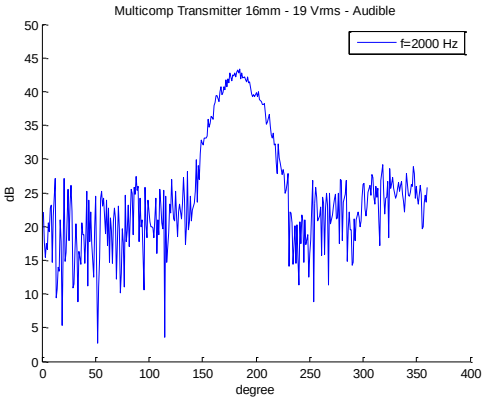

(j) 2 kHz – 19.75 V_{rms}

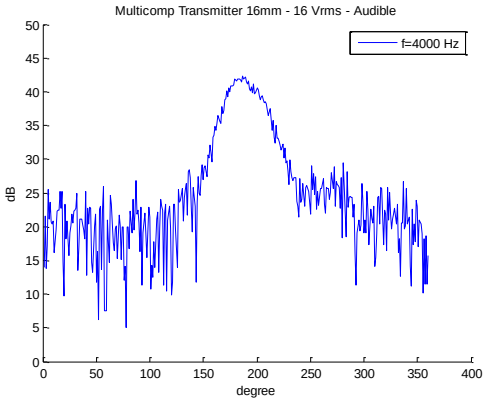

(k) 4 kHz – 16 V_{rms}

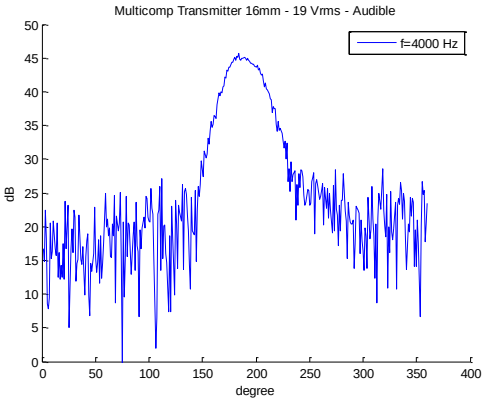

(l) 4 kHz – 19.75 V_{rms}

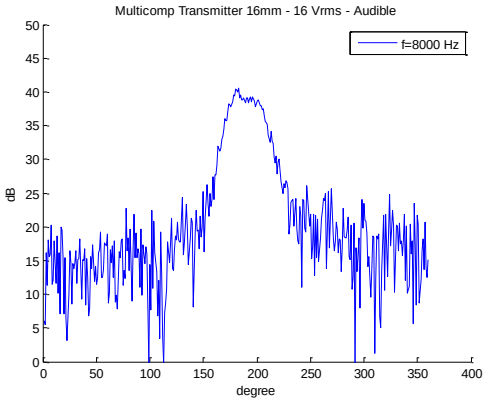

(m) 8 kHz – 16 V_{rms}

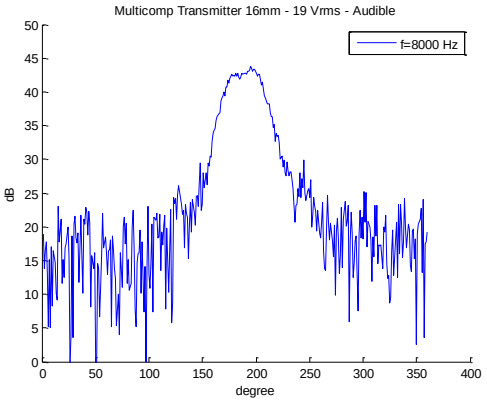

(n) 8 kHz – 19.75 V_{rms}

Figure 5.9. Directivity pattern of the resulting audible signals when the Multicomp 16 mm transducer is used with an input voltage of (a) 16 Vrms and (b) 19.75 Vrms. Octave frequencies from 125 Hz to 8 kHz are represented in independent figures.

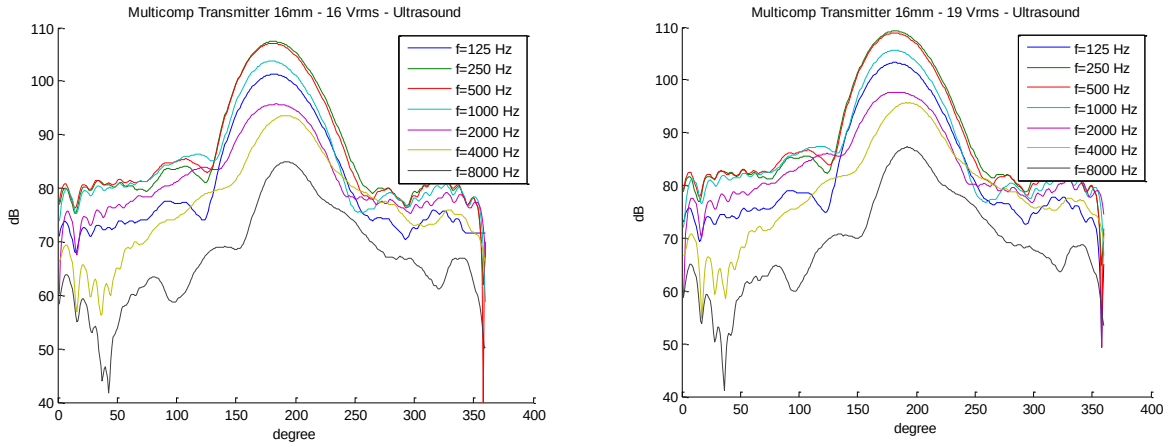

(a) 16 V_{rms} (b) 19.75 V_{rms}

Figure 5.10. Directivity pattern of the measured ultrasound levels (carrier frequency + octave-band central frequency) when the Multicomp 16 mm transducer is used with an input voltage of (a) 16 V_{rms} and (b) 19.75 V_{rms}. Octave-band frequencies from 125 Hz to 8 kHz are overlapped.

5.3.4 Transducer comparison

In Figure 5.11 the generated audible pressure for each transducer is represented in a single plot for each frequency and input voltage. Ultrasonic and carrier level comparisons are respectively shown in Figure 5.12 and Figure 5.13.

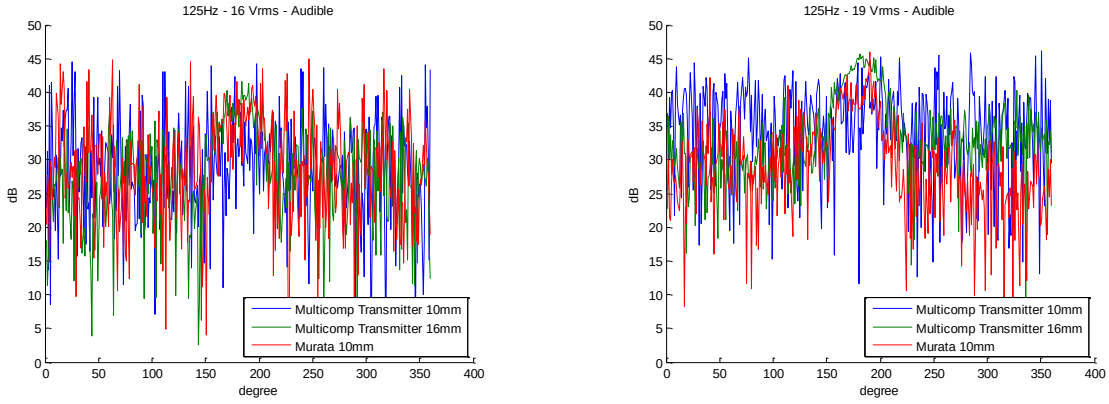

(a) 125 Hz – 16 V_{rms} (b) 125 Hz – 19.75 V_{rms}

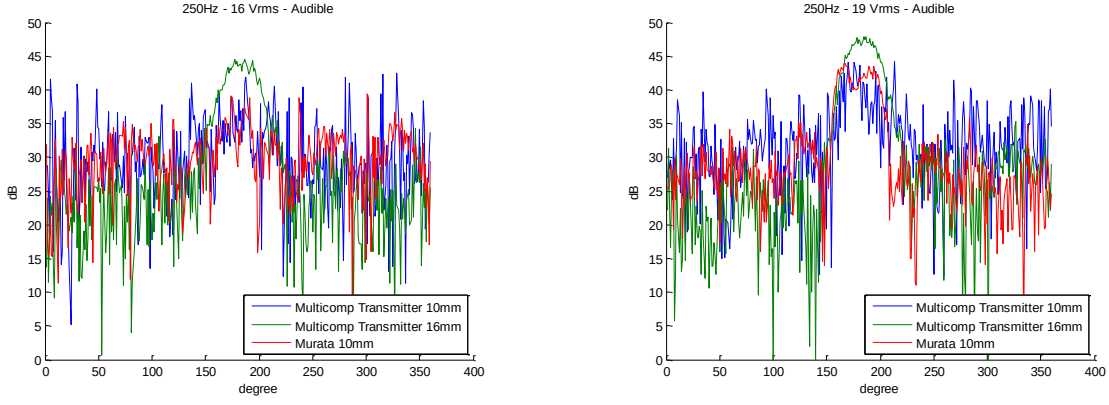

(c) 250 Hz – 16 V_{rms} (d) 250 Hz – 19.75 V_{rms}

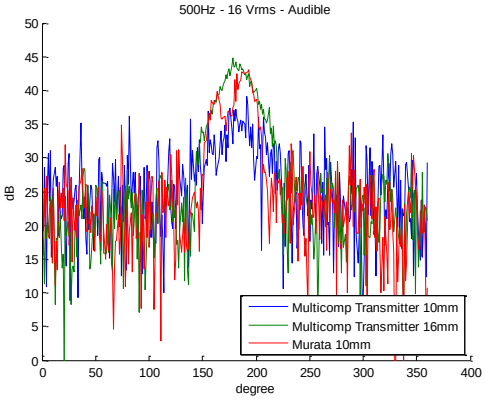

(e) 500 Hz – 16 V_{rms}

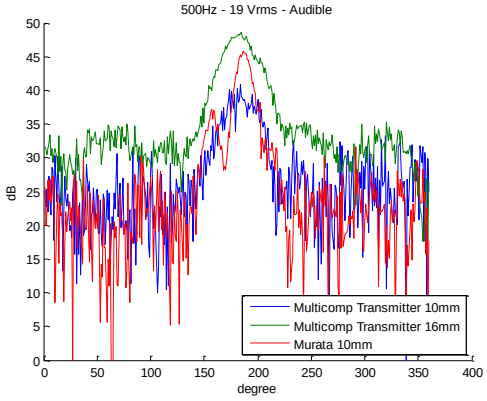

(f) 500 Hz – 19.75 V_{rms}

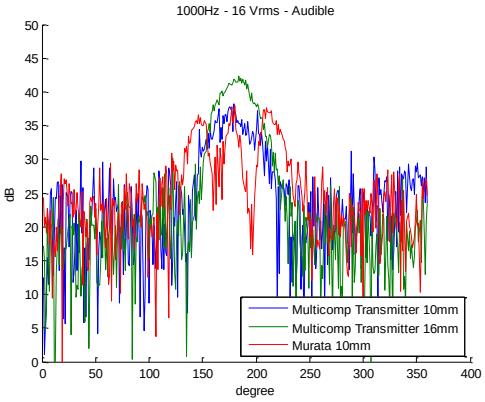

(g) 1 kHz – 16 V_{rms}

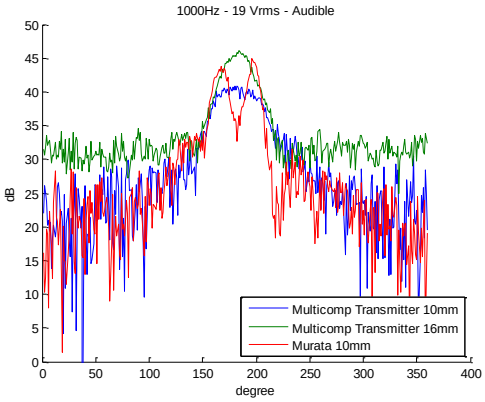

(h) 1 kHz – 19.75 V_{rms}

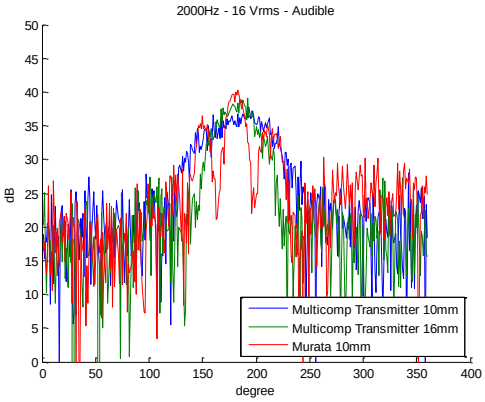

(i) 2 kHz – 16 V_{rms}

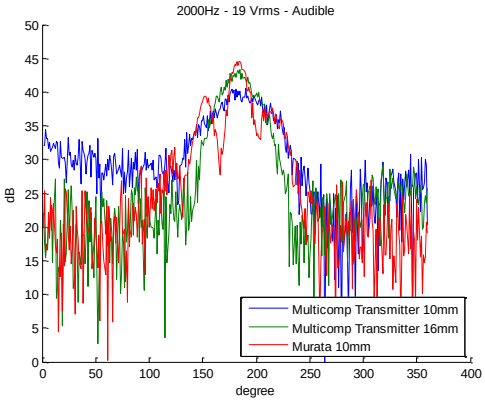

(j) 2 kHz – 19.75 V_{rms}

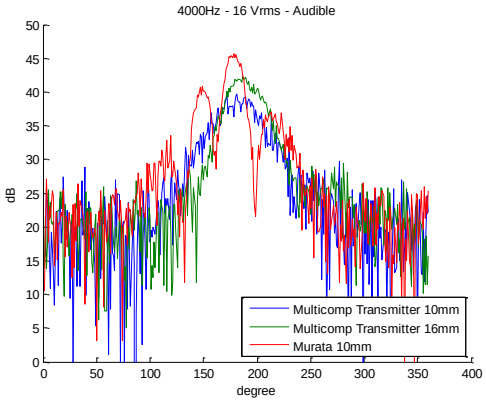

(k) 4 kHz – 16 V_{rms}

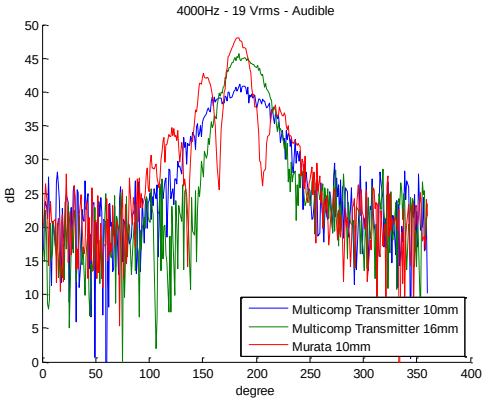

(l) 4 kHz – 19.75 V_{rms}

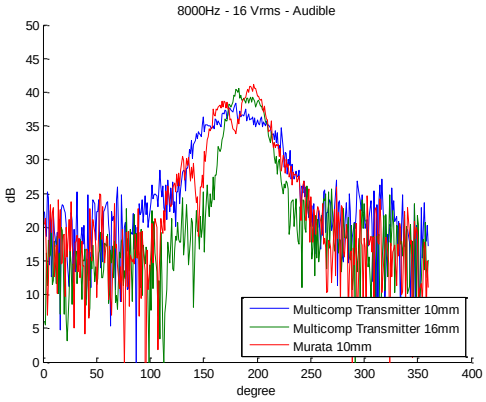

(m) 8 kHz – 16 V_{rms}

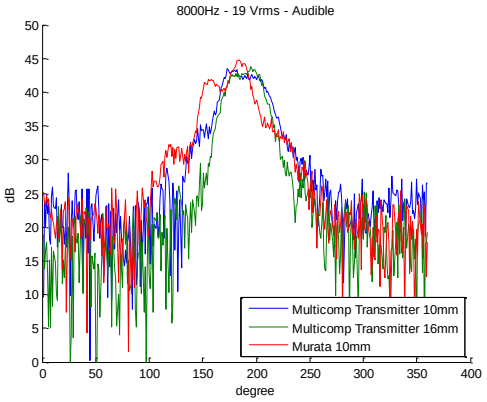

(n) 8 kHz – 19.75 V_{rms}

Figure 5.11. Directivity pattern of the resulting audible signals when the three different transducers are used with an input voltage of (a) 16 V_{rms} and (b) 19.75 V_{rms}. Octave frequencies from 125 Hz to 8 kHz are represented in independent figures.

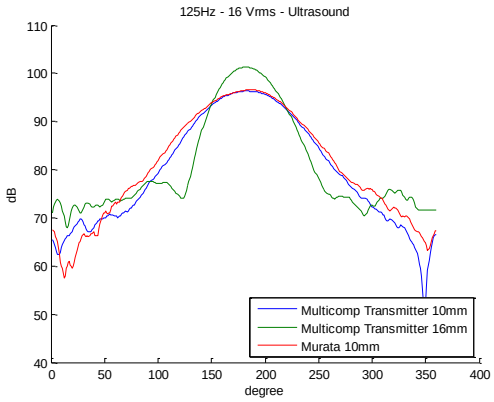

(a) 125 Hz – 16 V_{rms}

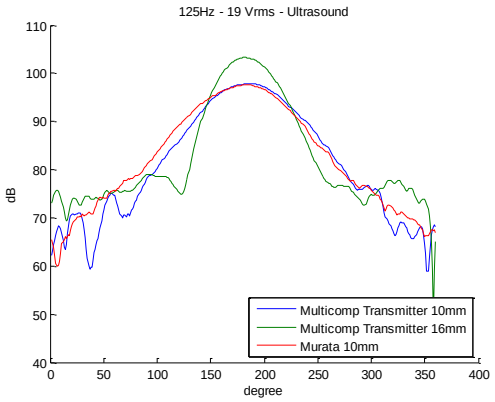

(b) 125 Hz – 19.75 V_{rms}

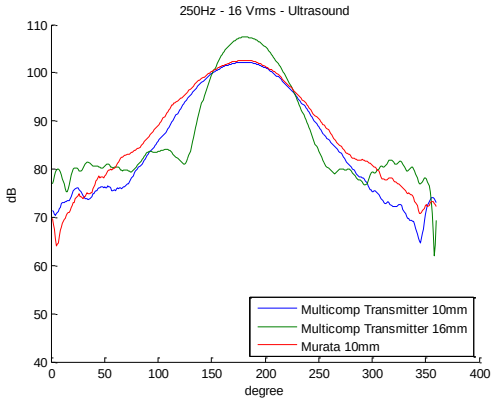

(c) 250 Hz – 16 V_{rms}

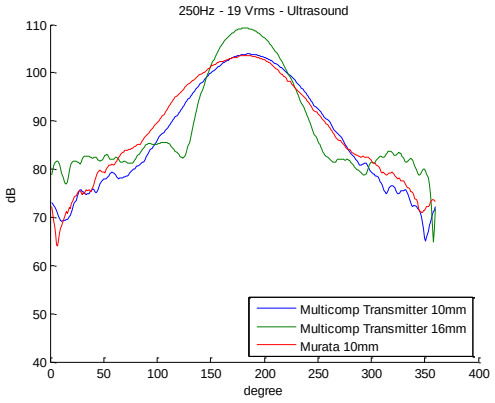

(d) 250 Hz – 19.75 V_{rms}

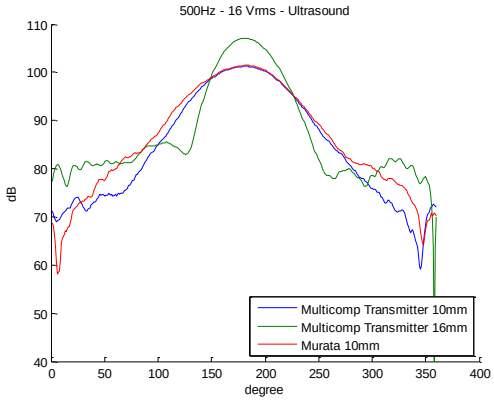

(e) 500 Hz – 16 V_{rms}

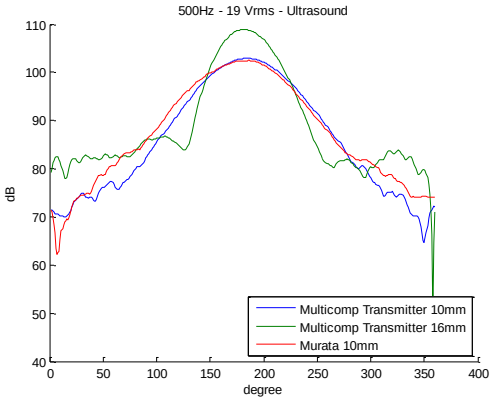

(f) 500 Hz – 19.75 V_{rms}

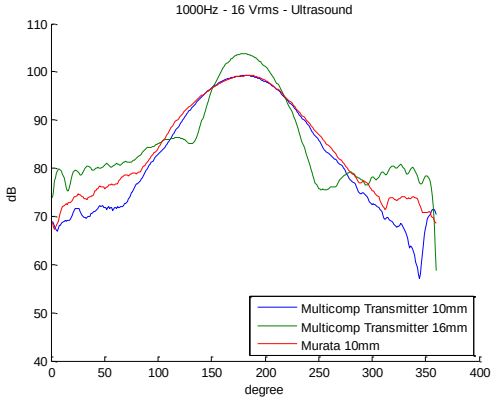

(g) 1 kHz – 16 V_{rms}

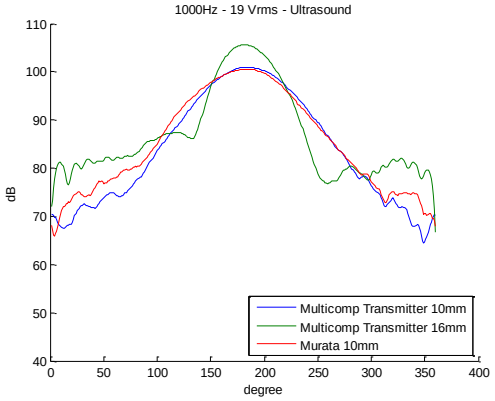

(h) 1 kHz – 19.75 V_{rms}

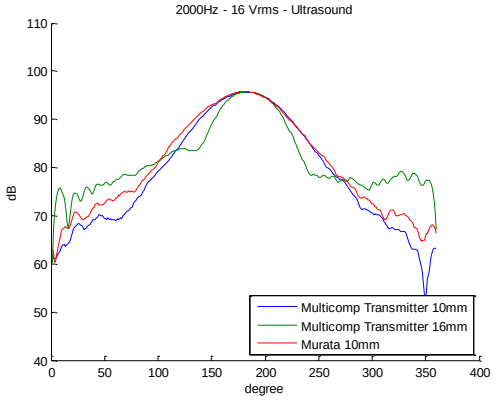

(i) 2 kHz – 16 V_{rms}

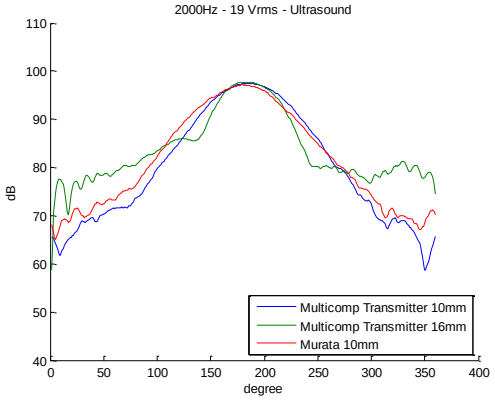

(j) 2 kHz – 19.75 V_{rms}

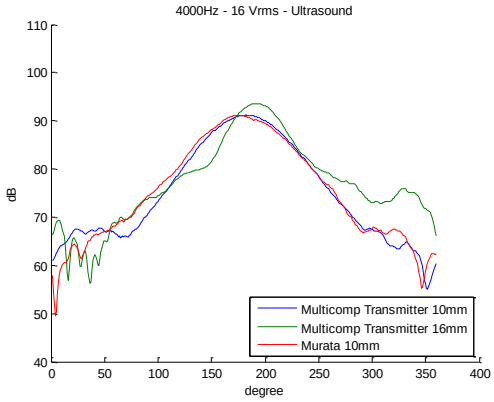

(k) 4 kHz – 16 V_{rms}

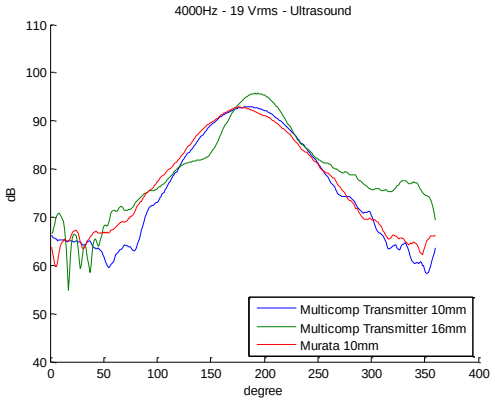

(l) 4 kHz – 19.75 V_{rms}

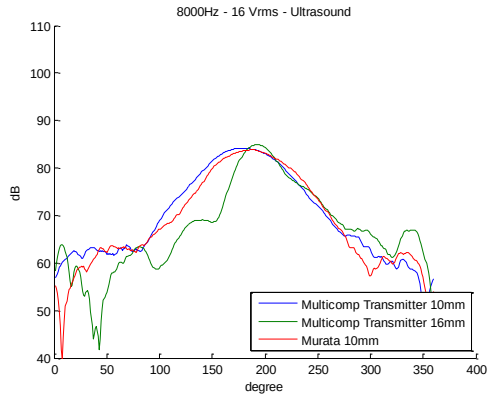

(m) 8 kHz – 16 V_{rms}

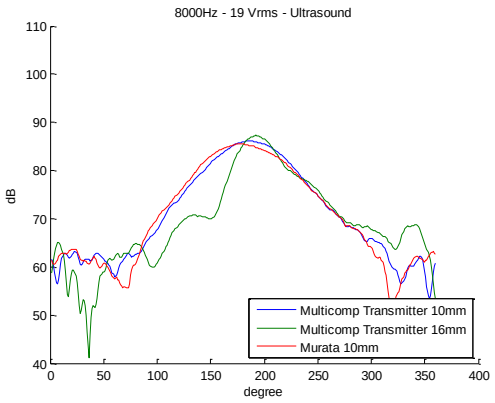

(n) 8 kHz – 19.75 V_{rms}

Figure 5.12. Directivity pattern of the measured ultrasound levels (carrier frequency + octave-band central frequency) when the three different transducers are used with an input voltage of (a) 16 V_{rms} and (b) 19.75 V_{rms}. Octave central frequencies from 125 Hz to 8 kHz are represented in independent figures.

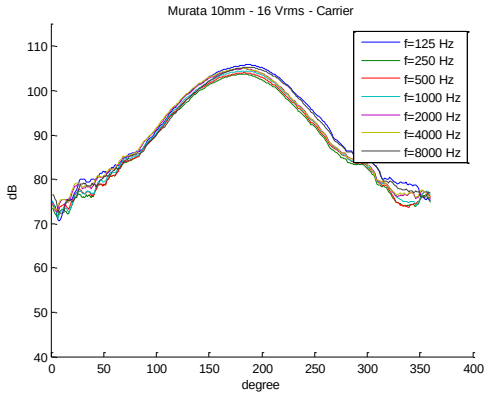

(a) Murata 10mm – 16 V_{rms}

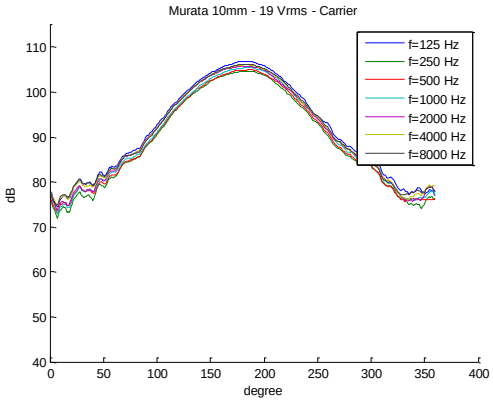

(b) Murata 10mm – 19.75 V_{rms}

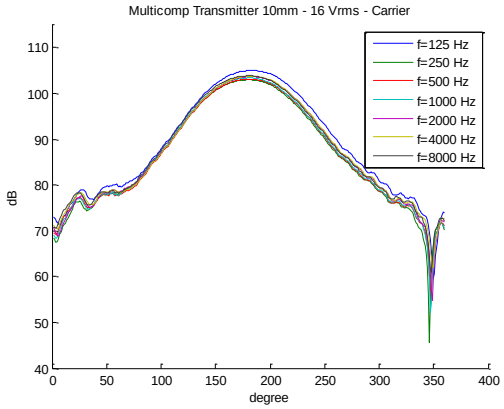

(c) Multicomp Transmitter 10mm – 16 V_{rms}

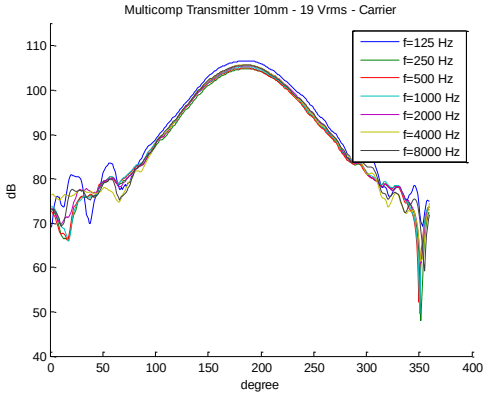

(d) Multicomp Transmitter 10mm – 19.75 V_{rms}

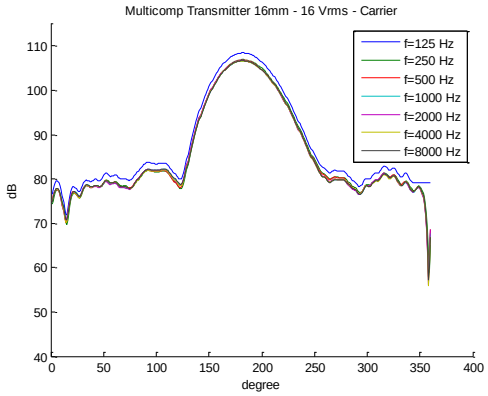

(e) Multicomp Transmitter 16mm – 16 V_{rms}

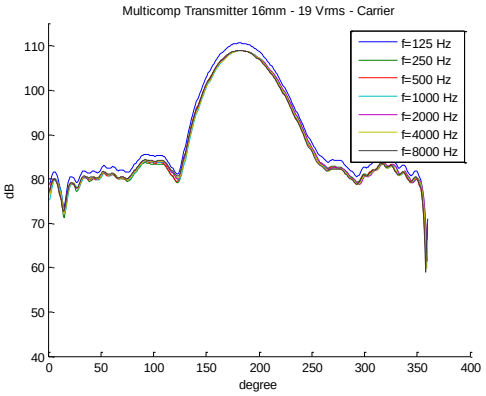

(f) Multicomp Transmitter 16mm – 19.75 V_{rms}

Figure 5.13. Directivity pattern of the measured carrier levels (40 kHz) when the three different transducers are used with an input voltage of (a) 16 V_{rms} and (b) 19.75 V_{rms}. Octave frequencies from 125 Hz to 8 kHz are overlapped.

5.4 Comparisons between theory and measurements

The improved theoretical model, detailed in D3.10, can predict the generated audible sound for a given directivity of the primary fields located in the ultrasonic frequency range (i.e., carrier levels and modulated sound). In what follows, the estimated audible sound is compared against measurements for each ultrasound transducer, using as inputs the experimental primary fields shown in the previous Section 5.3.

5.4.1 Murata 10mm Transmitter

Figure 5.14 shows the comparisons between the theoretical model and the measured audible sound for the Murata 10mm Transmitter. As it can be observed, a bad estimation of the audible sound is obtained. This is because this ultrasound transducer presents some unexpected side lobes in the audible range that are not present in the ultrasonic one (see Figure 5.4), which cannot be reproduced by the theoretical model.

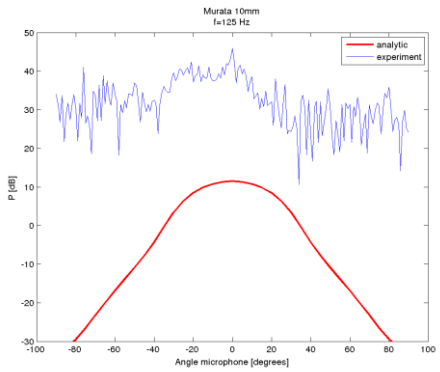

(a) 125 Hz

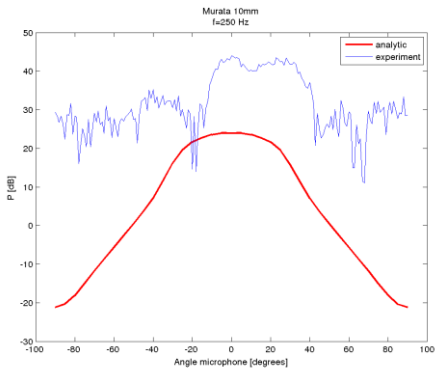

(b) 250 Hz

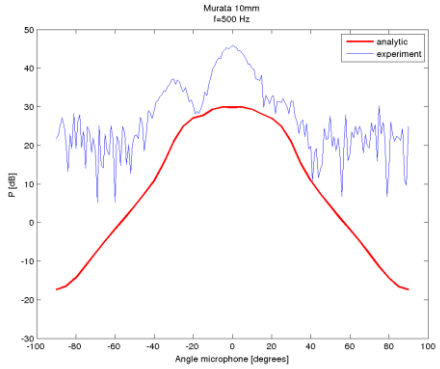

(c) 500 Hz

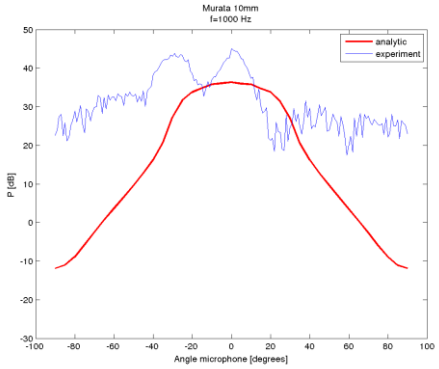

(d) 1 kHz

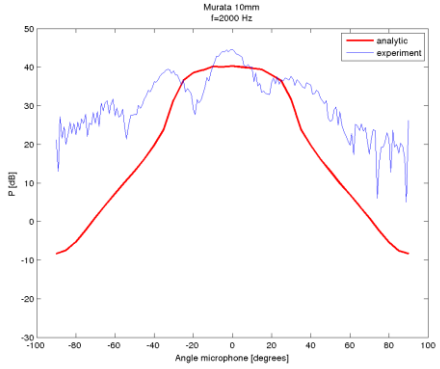

(e) 2 kHz

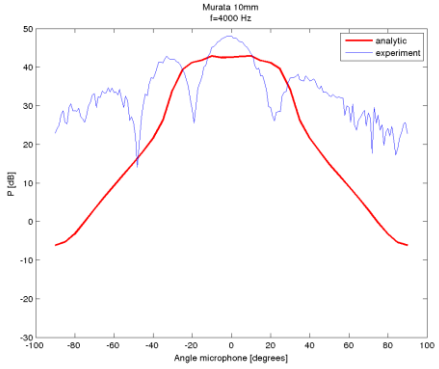

(f) 4 kHz

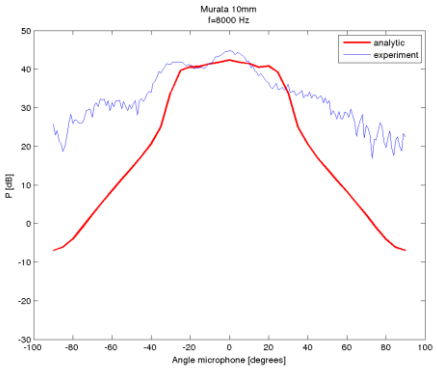

(g) 8 kHz

Figure 5.14. Comparison of the computed and measured directivity pattern for ultrasound transducer Murata 10mm Transmitter at different frequencies.

5.4.2 Multicomp 10mm Transmitter

Figure 5.15 shows the comparisons between the theoretical model and the measured audible sound for the Multicomp 10mm Transmitter. A better estimation is obtained for this transducer compared to the Murata 10mm (see Figure 5.14), although SPLs are underestimated in the low frequency range. However, one cannot make a fair comparison in this range (especially at 125 Hz and 250 Hz) because the experimental audible sound is masked by the background noise. This issue requires further investigation.

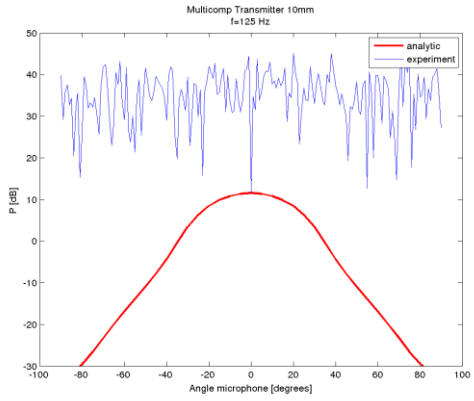

(a) 125 Hz

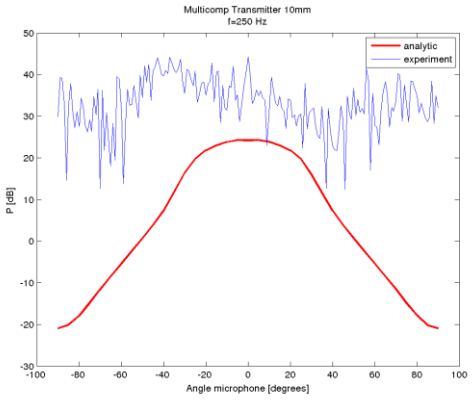

(b) 250 Hz

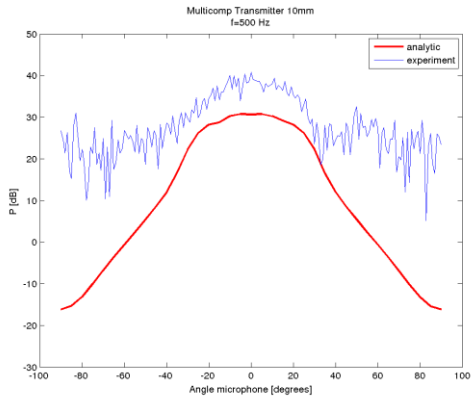

(c) 500 Hz

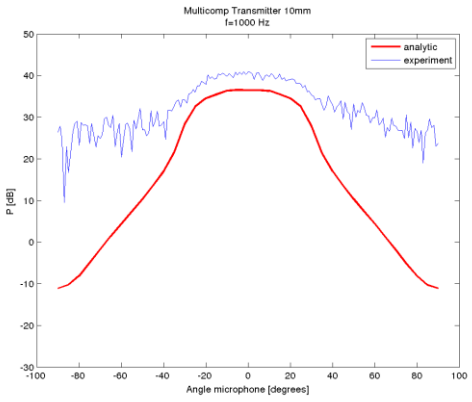

(d) 1 kHz

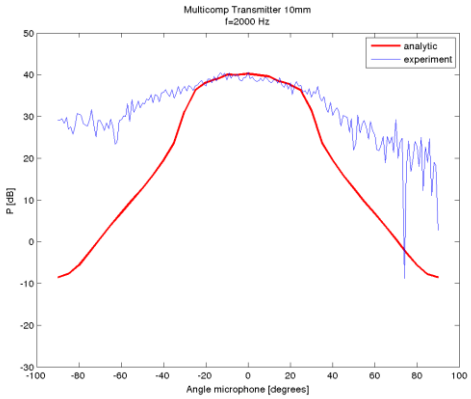

(e) 2 kHz

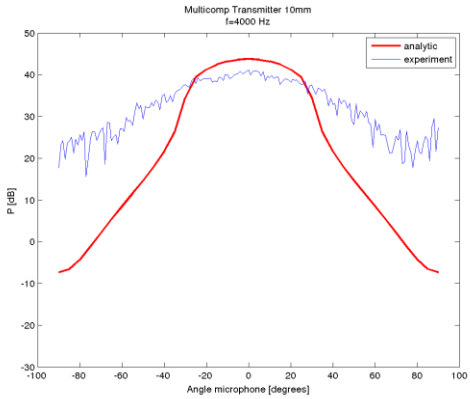

(f) 4 kHz

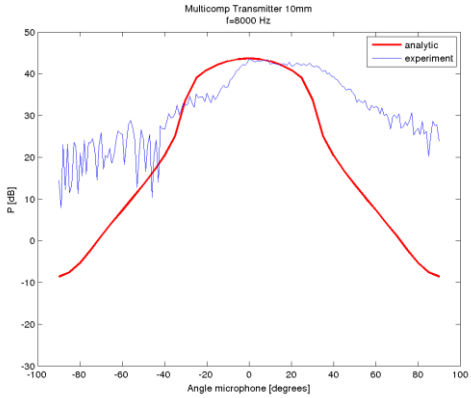

(g) 8 kHz

Figure 5.15. Comparison of the computed and measured directivity pattern for ultrasound transducer Multicomp 10mm Transmitter at different frequencies.

5.4.3 Multicomp 16mm Transmitter

Figure 5.16 shows the comparisons between the theoretical model and the measured audible sound for the Multicomp 16mm Transmitter. A very good matching is obtained for frequencies beyond 1 kHz. In contrast to the Multicomp 10mm Transmitter, for this transducer we get high enough SPLs at low frequencies so as to overcome the background noise. Unfortunately, SPLs are underestimated compared to experiments.

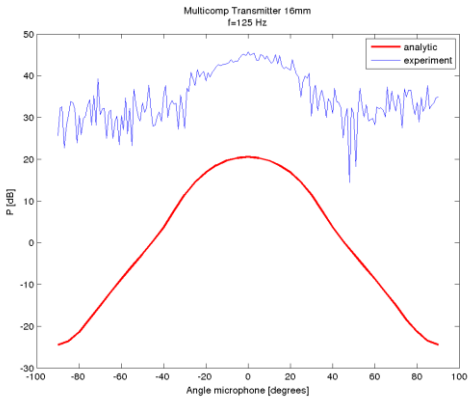

(a) 125 Hz

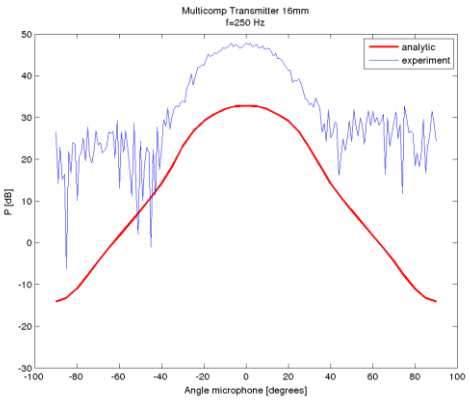

(b) 250 Hz

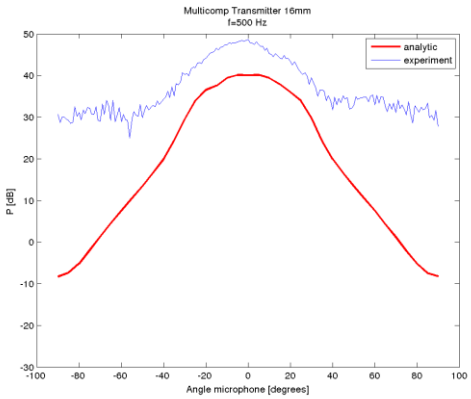

(c) 500 Hz

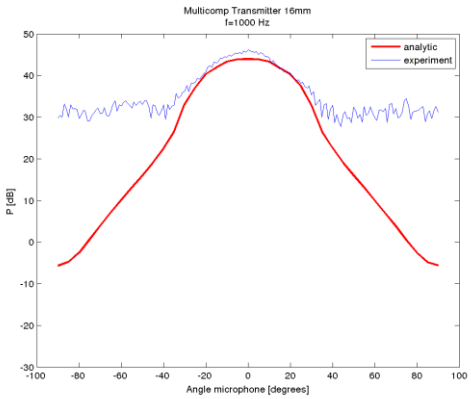

(d) 1 kHz

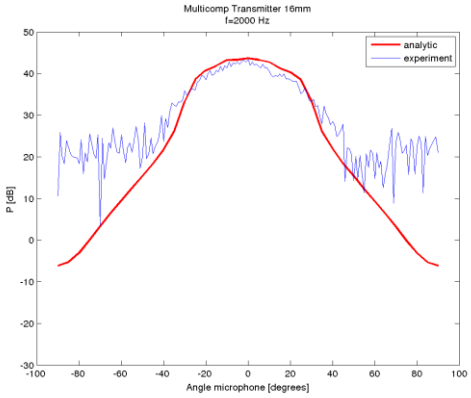

(e) 2 kHz

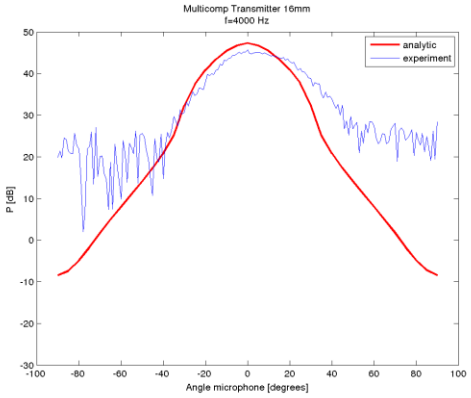

(f) 4 kHz

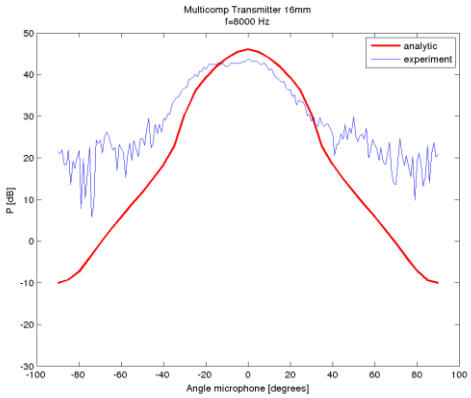

(g) 8 kHz

Figure 5.16. Comparison of the computed and measured directivity pattern for ultrasound transducer Murata 16mm Transmitter at different frequencies.

5.5 Conclusions

As expected, the transducers with a 10 mm diaphragm (Multicomp 10 mm and Murata 10 mm) have shown lower pressure values and a less directive nature than that with a bigger diaphragm (Multicomp 16 mm). Modifying the input voltages from 16 V_{rms} to 19.75 V_{rms} has also resulted in higher SPL for all the frequencies for both the audible and ultrasonic ranges. Any significant modification of the directivity shape has been detected when doing so. Regarding the carrier level, it can be considered constant throughout the frequency range.

As far as the transducer choice for the second OPL prototype (OPL#2) is concerned, the Murata 10 mm has been discarded because it has a strange behaviour that cannot be predicted by the theoretical model. It presents some unexpected side lobes in the audible frequency range, while any of them were present in the ultrasonic one. The Multicomp 10 mm was also discarded because it could not generate audible SPLs higher than the background noise at low frequencies. The Multicomp 16 mm seems then to be the best candidate for the construction of the OPL#2. It gives the highest SPLs for all the audible frequency range. Moreover, the theoretical model provides a very good estimation of the generated audible field, although for low frequencies (<1 kHz) the SPLs were underestimated. For this range the predicted values should be read as a lower bound.